NASA TM X- 63324

THE SOLAR CONSTANT AND THE SOLAR SPECTRUM MEASURED FROM A RESEARCH AIRCRAFT AT 38,000 FEET

GPO PRICE $ _____

CSFTI PRICE(S) $ _____

Hard copy (HC) 3.00

Microfiche (MF) .65

ff 653 July 65

AUGUST 1968

GSFC

GODDARD SPACE FLIGHT CENTER

GREENBELT, MARYLAND

FACILITY FORM 602

N68-34697 (ACCESSION NUMBER)

(THRU)

69 (PAGES)

1 (CODE)

TMX-63324 (NASA CR OR TMX OR AD NUMBER)

29 (CATEGORY)

X-322-68-304

THE SOLAR CONSTANT AND THE SOLAR SPECTRUM MEASURED FROM A RESEARCH AIRCRAFT AT 38,000 FEET

by

Thermodynamics Branch, Test and Evaluation Division
and
Thermophysics Branch, Spacecraft Technology Division

August 1968

GODDARD SPACE FLIGHT CENTER
Greenbelt, Maryland

THE SOLAR CONSTANT AND THE SOLAR SPECTRAL IRRADIANCE MEASURED FROM A RESEARCH AIRCRAFT AT 38,000 FEET

The NASA 711 Galileo Experiment
August 1967

Management and Experimenters Team
Goddard Space Flight Center

Dwight C. Kennard, Jr., Head, Research and Technology Office, T. & E. Divn., Project-Manager.

Matthew P. Thekaekara, Principal Investigator, Perkin-Elmer, P-4 Interferometer.

Raymond Kruger, Head, Space Simulation Research Section, Project Coordinator, Acting Project Manager at Ames Research Center—Cone Radiometer, Mounting Fixtures.

Charles H. Duncan, Head, Radiometry Section, Assistant Project Manager—Ångström 7635, Thermophysics Branch Experiments.

John F. Rogers, Assistant Project Manager—P-4 and I-4 Interferometers, Flight Paths, Mounting Fixtures.

Ralph Stair, (Senior Scientist, Neotec Corporation, Rockville, Md.) Consultant—Filter Radiometer, Perkin-Elmer, Data Analysis.

James J. Webb—Electronic Scanning Spectrometer, Ångström 7635, Thermophysics Branch Experiments.

Roy McIntosh—Leiss Monochromator, Thermophysics Branch Experiments.

Patrick Ward—P-4 and I-4 Interferometers.

Antony J. Villasenor—Computer Programs for P-4 and I-4 Interferometers and Perkin-Elmer.

Robert J. Maichle—Electronics, Tape Recorder, Time Code Generator, Signal Calibration.

Arthur McNutt—Ångström 6618, Hy-Cal, Eppley Normal Incidence Pyrheliometers.

Arthur R. Winker—Perkin-Elmer, Thermodynamics Branch Experiments.

Thomas A. Riley—Ångström 6618, Hy-Cal, Eppley Normal Incidence Pyrheliometers.

Daniel L. Lester—Filter Radiometer, Thermophysics Branch Mounting Fixtures.

Segun G. Park—Leiss Monochromator, Thermophysics Branch Mounting Fixtures.

Cooperating Team, Cary 14 Monochromator, John C. Arveson, Roy N. Griffin and Bart T. Kinney, Ames Research Center.

Airborne Sciences Office Personnel.

Michael Bader, Chief, Airborne Sciences Office.

Robert M. Cameron, Test Coordinator.

Roy L. Adkins, Pilot.

Jack Kroupa, Navigator.

Glen Stinnet, Co-pilot.

Frank Brasmer, Senior Flight Engineer.

B. B. Gray, Flight Engineer.

Dave Shute, Sun Compass.

Milton Henderson, Sun Compass.

James Cox, Aircraft Maintenance.

CONTENTS

THE SOLAR CONSTANT AND THE SOLAR SPECTRUM MEASURED FROM A RESEARCH AIRCRAFT AT 38,000 FEET

by
Thermodynamics Branch, Test and Evaluation Division
and
Thermophysics Branch, Spacecraft Technology Division
Goddard Space Flight Center

PART I

THE AIRBORNE SOLAR IRRADIANCE OBSERVATORY

M. P. Thekaekara and R. Kruger

1. THE FLYING OBSERVATORY PROJECT

Three groups of experimenters of the National Aeronautics and Space Administration undertook in August 1967 a combined project to measure the solar constant and solar spectral irradiance from a research airplane flying at 38,000 feet. Two of the groups were from Goddard Space Flight Center, Greenbelt, Maryland, which initiated the project, and the third from Ames Research Center, Moffett Field, California. The flights were made from Moffett Field. The airplane was fitted out as a high altitude solar irradiance laboratory, with twelve different instruments, seven for spectral and five for total irradiance. The instruments represented a wide variety of measuring techniques and incorporated some of the best available features in precision radiometry.

The solar constant is the amount of total solar energy of all wavelengths received per unit time per unit area exposed normally to the sun's rays at the average distance of the earth in the absence of the earth's atmosphere. The solar spectral irradiance is the distribution of the same energy in narrow spectral bands. Our present knowledge of these physical quantities is based mainly on ground-based measurements. Most of the pioneering work was done by the Smithsonian Institution, Washington, D. C., which gathered extensive data over a period of 50 years up to 1955.

The value of the solar constant most often quoted, at least in the United States, is 2.00 calories per square centimeters per minute. This value was deduced by Francis S. Johnson[1] at the Naval Research Laboratory, Washington, D. C. in 1954. It is interesting to note that the solar constant has frequently been revised, and most revisions have yielded a higher value than those accepted previously. Some of the more significant revised values are given in Table 1.

Table 1

Significant Revisions of the Solar Constant.

Author	Year	Solar Constant cal cm^{-2} min^{-1}
P. Moon[2]	1940	1.896
L. B. Aldrich and G. C. Abbot[3]	1948	1.90
W. Schuepp[4]	1949	1.96 to 2.03
C. W. Allen[5]	1950	1.97
L. B. Aldrich and W. H. Hoover[6]	1952	1.934
F. S. Johnson[1]	1954	2.00
C. S. Allen[7]	1955	1.97 $\pm$ .01
R. Stair and R. G. Johnston[8]	1956	2.05
C. W. Allen[9]	1958	1.978

The latest published value which can be quoted with some degree of confidence is that given by C. W. Allen[9] in his Symons Memorial Lecture of 1958. He gives a table of values and a curve of the solar spectrum outside the earth's atmosphere, and derives from it the value of the solar constant to be 1.978 cal-cm^{-2} min^{-1}. In this work he reconsidered his earlier data[5] with the help of discussions by Deirmendjian and Sekera,[10] Johnson, Purcell, Tousey and Wilson,[11] and Johnson.[1] Some account was also taken of the measurements of the intensity at the center of the solar disc in the continuum between Fraunhofer lines by Makarova,[12] Peyturaux[13] and Labs.[14]

Table 1 shows that the values of the solar constant given in literature vary from 1.90 to 2.05 cal cm^{-2} min^{-1}. Most authors agree that the irradiance due to the sun at the sun-earth distance is in itself highly constant. The disagreements between authors is due largely to the difficulties of making measurements through the highly variable smoke, dust, haze and cloud cover of the earth's atmosphere.

The discrepancies between different investigators are even greater for solar spectral irradiance. Tables of solar spectral data have been published by Moon,[2] Johnson,[1] Stair and Johnston,[8] Allen[9] and others. Some of the more significant data have been collated and published by Gast[15] in the "Handbook of Geophysics," where he makes the following observation. "As an example of a more important uncertainty, in the ultraviolet region (300 to 359 mμ), the discrepancy between various observations is about 10 percent, and there have been reported variant observations as large as 40 percent which can be neither ignored nor explained." Dunkelman and Scolnik[16] have published charts which show these differences in a striking manner. It is seen that at 3400Å Petit's value is about 4 times that of Gotz and Schonman, and at 6000Å the Smithsonian value is 40 percent higher than that of Reiner. Even more discouraging is the difference between relatively recent measurements, as for example, between Stair and Johnston and Dunkelman and Scolnik. A detailed report on the state of our knowledge of the solar constant and solar spectral irradiance has been published by M. P. Thekaekara.[17]

The uncertainties in our presently accepted values for spectral irradiance are considerably greater than for the total irradiance. In the wavelength range beyond 0.7 μ where the atmospheric water vapor bands are many and strong, most authors, following P. Moon, have assumed the solar spectrum to be that of a 6000°K blackbody. The wide differences between authors in the shorter wavelength range and the relative lack of experimental data in the longer wavelength range strongly

indicated the need of a new method which is free of many of the uncertainties of ground based measurements. Hence it was that the NASA 711 project was undertaken.

At the flight altitude of 38,000 feet the observers were above nearly 80 percent of the permanent gases of the atmosphere, and more importantly above nearly 99.9 percent of the water vapor and all the dust and smoke which form the highly variable and absorbent constituent of the atmosphere. The combination of 12 different instruments, complimenting each other in wavelength range, spectral resolution and measuring techniques, calibrated and operated by different experimenters, and borne in an airborne laboratory at 38,000 feet, practically free of atmospheric absorption, is considered a valuable feature in enhancing the level of confidence in the final result.

This present report gives the results from eleven of the instruments, those operated by the two GSFC groups. The Ames monochromator was flown also in several later flights of the aircraft, and its results will be reported later in a separate publication. This report consists of three parts. The first part describes the project as a whole, the airborne solar irradiance laboratory, general features of the instrumentation, the flight paths, atmospheric correction techniques and associated problems common to all the flight experiments. The second and third parts discuss the measurements of total and spectral irradiance respectively. These instruments were operated by the Thermodynamics Branch, Test and Evaluation Division and the Thermophysics Branch, Spacecraft Technology Division. The experimental procedure, data analysis and results of each instrument will be discussed by the persons who operated them. In conclusion, combining the results of the eleven instruments we shall present a new value of the solar constant and a new solar spectral irradiance curve for zero air mass.

2. THE AIRCRAFT AND THE EXPERIMENTS

The aircraft was a NASA-owned four-engine jet, NASA 711 Galileo, commercially known under its model name Convair 990. The team for solar irradiance measurements consisted of 18 experimenters, scientists and technicians to operate the instruments and 9 aircraft personnel. An inflight view of the aircraft is shown in Figure 1. Prominent among the special features which make it an air-borne science laboratory are the large extra windows on the roof of the plane and the replacement of some of the passenger windows by optical quality material. Other special features are electrical power outlets at each experimenter's station, defrosters for observation windows, time code generator, and precise navigational equipment for the determination of latitude, longitude and solar zenith angle.

Figure 2 is a photograph giving a view of the front section, left side of the plane. It was taken while the plane was in the hangar. The figure shows clearly four of the passenger windows where the double plexiglass cover has been replaced by aluminum plates with small apertures in them. The apertures are covered by optical material suited to the instrument behind each window.

The location of each of the experiments is shown in Figure 3. The instruments for observing the sun are on the left side of the aircraft, as also some of the electronics chassis and chart

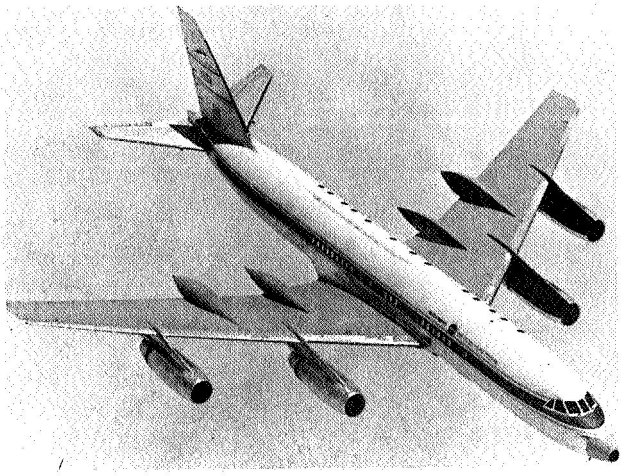

Figure 1—NASA 711, Galileo, Convair 990A, the airborne laboratory in flight.

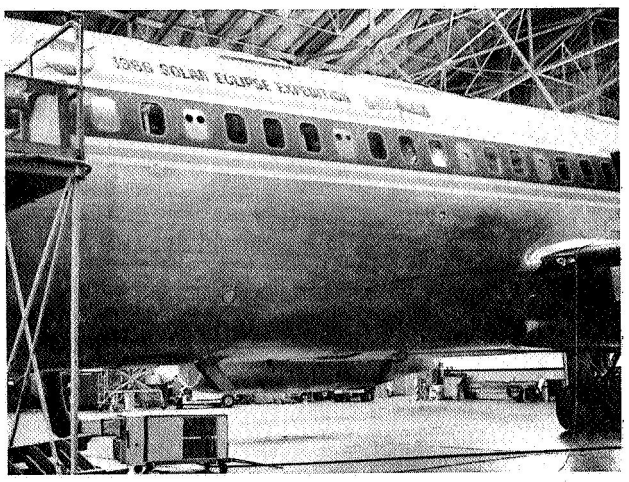

Figure 2—NASA 711, port side view, showing passenger windows changed to observation ports.

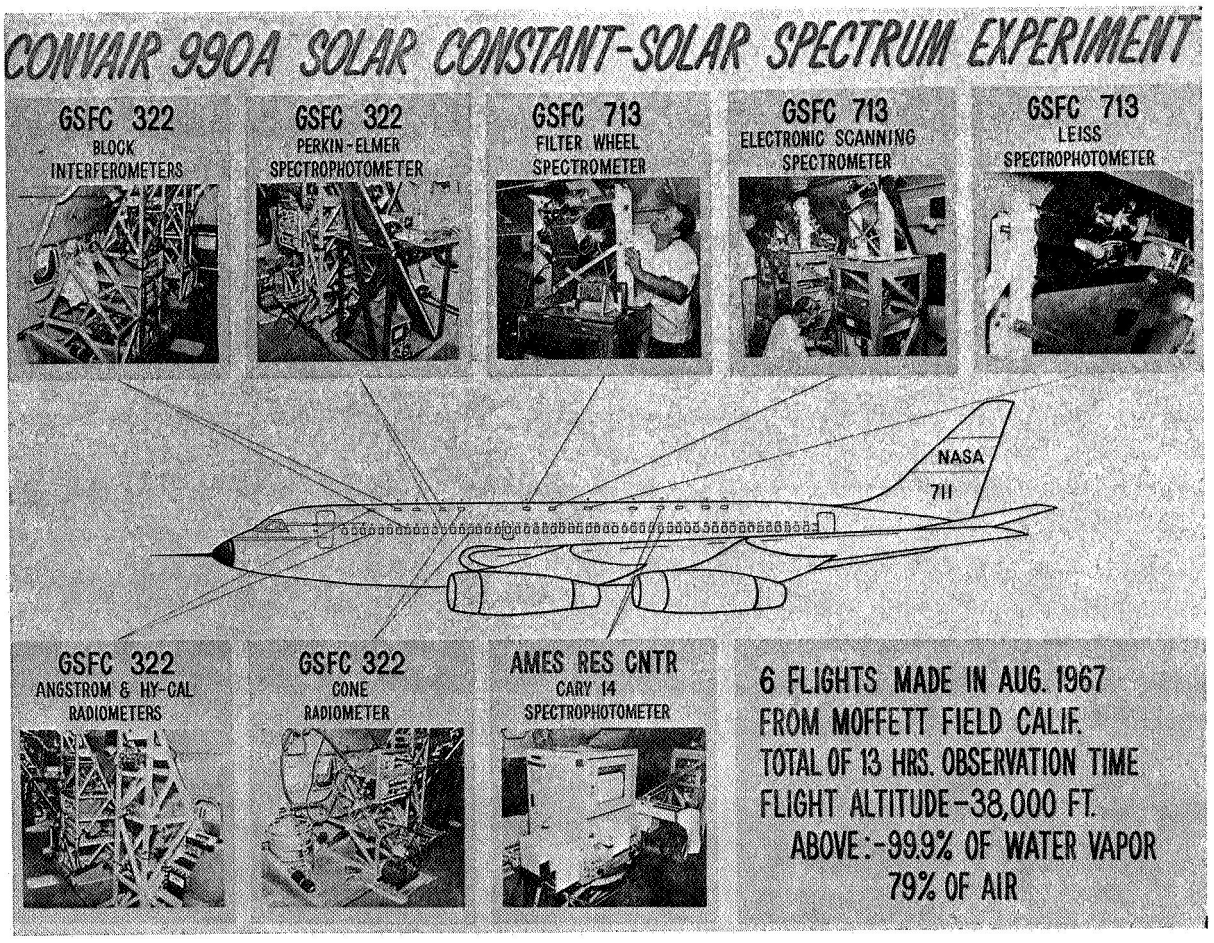

Figure 3—NASA 711, location of on-board experiments.

Table 2

Data on Instruments Used for Solar Irradiance Measurements
Onboard NASA 711 Galileo

August 1967

Instruments	Energy Detector	Type of Instrument	Aircraft Window Material	Wavelength Range	Experimenters
1 Hy-Cal Pyrheliometer	Thermo-electric emf	Total	Infrasil	0.3 to 4 μ	McNutt, Riley
2 Ångström Pyrheliometer 6618	Resistance Strip	Total	Infrasil	0.3 to 4 μ	McNutt, Riley
3 Eppley Normal Incidence Radiometer	Thermo-electric emf	Total	Infrasil	0.3 to 4 μ	McNutt, Riley
4 P-4 Interferometer	1P28 or R136 PbS Tube	Soleil Prism Soleil Prism	Infrasil Infrasil	0.3 to 0.7 μ 0.7 to 2.5 μ	Rogers, Ward
5 I-4 Interferometer	Thermistor Bolometer	Michelson's Bi-mirror	Irtran 4	2.6 to 15 μ	Ward, Rogers
6 Perkin-Elmer Monochromator	1P28 Tube Thermocouple	LiF Prism LiF Prism	Sapphire Sapphire	0.3 to 0.7 μ 0.7 to 4 μ	Thekaekara, Winker, Stair
7 Cone Radiometer	Resistance Wire	Total	Infrasil	0.3 to 4 μ	Kruger, Winker, Ward
8 Filter Radiometer	Phototube	Dielectric Thin Film Filters	Dynasil	0.3 to 1.2 μ	Stair, Lester
9 Ångström Pyrheliometer 7635	Resistance Strip	Total	Dynasil	0.3 to 4 μ	Duncan
10 Electronic Scanning Spectrometer	Image Dissector Tube	Grating	Dynasil	0.3 to 0.48 μ	Webb
11 Leiss Monochromator	E. M. I. 9558 Q. A. PbS Tube	Quartz Double Prism	Dynasil	0.3 to 0.7 μ 0.7 to 1.6 μ	McIntosh, Park, Stair
12 Cary 14 Monochromator	1P28 Tube PbS Tube	Grating and Prism	Dynasil	0.3 to 0.7 μ 0.7 to 2.5 μ	Arveson, Griffin, Kinney

recorders. To the right of the aircraft are located the tape recorders and the larger electronic equipment, namely, those for the three monochromators. A listing of the instruments in the order in which they were located, starting from the front of the airplane, is given in Table 2, as also some basic summary data on each. These instruments were selected partly because they had all been tested and believed to be sufficiently reliable at levels of solar irradiance, and partly because they could be readily mounted and operated on an airplane almost as well as in the laboratory. A general description of the instruments will be attempted here, in order to bring out the specific function of each and their distinguishing characteristics, and to show how being based on different techniques they complement each other.

Five of the instruments are for measuring the total irradiance, namely, Hy-Cal, Eppley, Cone and the two Ångströms; the others are for spectral irradiance. The Hy-Cal and Eppley are

instruments to measure the radiation in terms of the thermo-electric e.m.f. generated by them; conversion to units of irradiance is by means of the calibration supplied along with the instruments. The calibration is with reference to standards maintained by the respective manufacturers, the Hy-Cal Engineering Company, Santa Fe Springs, Cal. and the Eppley Laboratories, Newport, Rhode Island. The primary standard for the Hy-Cal is a blackbody and for the Eppley the international pyrheliometric scale. The two Ångström radiometers were also obtained from the Eppley Laboratory, and are distinguished by their serial numbers. The principle of measurement is that of balancing the resistance of two metal strips one of which is exposed to radiation and the other heated by an electric current. The calibration is with reference to the international pyrheliometric scale. The Cone radiometer is an absolute instrument which was designed and developed in the Thermodynamics Branch, GSFC. The irradiance is known from the difference in electrical heating power supplied to the wire-wound cone with and without the external radiation. The angular aperture of these instruments is limited by the diaphragm mounted in front of each at some distance away from the sensitive surface, so that the incident energy is due only to the sun and a known small fraction of the circumsolar sky. The irradiance of the circumsolar sky at 38,000 feet was computed from data published in literature[18] to be about 5×10^{-4} (1/20 percent) of that of the sun. In Table 2 the wavelength range of these instruments is given as .3 to 4 μ, the lower limit being due to the ozone and the upper limit to the quartz window of the aircraft.

There were seven instruments for measuring the spectral distribution of solar irradiance. They represent a wide variety of size, design, construction, measuring process, data analysis, wavelength range and resolution. There are three monochromators, Perkin-Elmer (Perkin-Elmer Corporation, Norwalk, Conn.), Leiss (Leiss Instrument Co., West Germany), and Cary 14 (Cary Instruments, Monrovia, Cal.); two interferometric spectrometers (Block Engineering, Inc., Cambridge, Mass.), the P-4 for the range up to 2.5 μ and the I-4 for the IR range up to 15 μ, one electronic scanning spectrometer (I. T. T., Fort Wayne, Ind.); and a filter radiometer designed and constructed by the Thermophysics Branch, GSFC. The wavelength range covered by the instruments was determined by the material of the dispersive element and by the detector. The visible range .3 to .65 μ was scanned by all instruments except the I-4. Photomultipliers are highly sensitive in this range. The near IR, .7 to 2.5 μ was covered by Leiss, P-4, Cary 14 and partly also by the filter radiometer. The detector was a phototube for the filter radiometer and PbS cells for the other three. The Perkin-Elmer having an LiF prism and thermocouple detector covered the range up to 4 μ. The I-4 interferometer spanned the range 2.6 to 15 μ. The material for the aircraft window was selected according to the range covered by the respective instrument, Irtran 4 for I-4, sapphire for Perkin-Elmer and fused quartz for the others. For the five instruments to the rear of the aircraft the entire window was covered by a quartz plate, grade Dynasil 4000, size 12" × 14", thickness 1"; these windows were available from earlier solar eclipse expeditions of NASA 711. The observation windows in the front were covered by aluminum blanks with circular holes of 4" diameter for infrasil quartz or sapphire and of 2" diameter for Irtran-4. These windows were made specifically for these solar irradiance flights. The infrasil ensured better transmittance in the H_2O bands and the small apertures lessened the scattered light within the aircraft. The pointing accuracy of the instruments towards the sun was ensured in azimuth by the aircraft itself which maintained a flight path constantly at right angles to the sun. Accuracy in elevation

was ensured for the Perkin-Elmer and Cary 14 by external reflecting optics which tracked the changing elevation of the sun, and for the other 10 instruments by the instrument itself rotating about a horizontal axis parallel to the length of the aircraft. For the instruments 8 through 11, the fixture design permitted observation through the upper windows only. The other instruments could be shifted to the lower windows for low solar elevation. The normal to these windows was at 65° to the horizontal for the upper windows and at 14° to the horizontal for the lower windows.

The spectral irradiance instruments display a wide diversity in their principle of operation and their data acquisition and analysis. The three monochromators, though greatly different in external and internal optics have in common a dispersing element. In the filter radiometer 30 narrow band filters are interposed in succession between the incoming light and the detector. The electronic scanning spectrometer operates on a principle similar to the Vidicon camera, the spectrum is displayed on an X-Y plotter. The P-4 and I-4 record an interferogram on a magnetic tape from which later a spectrum is obtained by computerized Fourier analysis.

All spectral irradiance measurements are on a relative scale, since the output at any given wavelength depends not only on the incoming light but also on the transfer function of the instrument which is dependent on the wavelength. The transfer function is determined by measuring a standard of known spectral irradiance. The most reliable standards available at present in the range .25 to 2.5μ are the 1000 w quartz iodine lamps. They were formerly issued by the National Bureau of Standards and are now being issued by the Eppley Laboratories. For extending the wavelength range beyond 2.5μ two black-body sources were used, one operating in the temperature range 800° to 1400°K, manufactured by Infrared Industries, Santa Barbara, Cal., and the other operating in the temperature range 1700° to 3000°K, manufactured by Astro-Industries, Santa Barbara, Cal.

3. MOUNTING AND FIXTURE DESIGN OF THE INSTRUMENTS

All the instruments for total and spectral irradiance are as seen above, standard items of a radiometric laboratory. All of them, except the I-4 Michelson-type interferometer which required a special shockproof mounting, were also relatively insensitive to the levels of shock and vibration encountered on an aircraft. Only minor modifications were needed in the instruments themselves to change them from measurement of laboratory sources to that of the sun. However, for several months prior to the flight a major effort in design and construction was needed to provide for each instrument and each item of equipment a mount which would meet the specifications of the aircraft for loading and safety. Loads are borne by the two pairs of rails on either side which in ordinary passenger planes serve as the seat tracks. All mounting frames and instruments were attached to these rails either directly or with a one-inch plywood pallet. For the instruments operated by the Thermodynamics Branch Nos. 1 to 7 in Table 2 the design of the mounts and racks and a detailed stress analysis was undertaken by Fairchild-Hiller, Germantown, Maryland.[19] Fairchild-Hiller Corporation built the instrument mounts; the electronics racks were built in the GSFC Fabrication Division. The design and fabrication of the mounts for instruments which were operated by the Thermophysics Branch, Nos. 8 to 11, was done jointly by Metcraft, Inc., Baltimore, Maryland, and

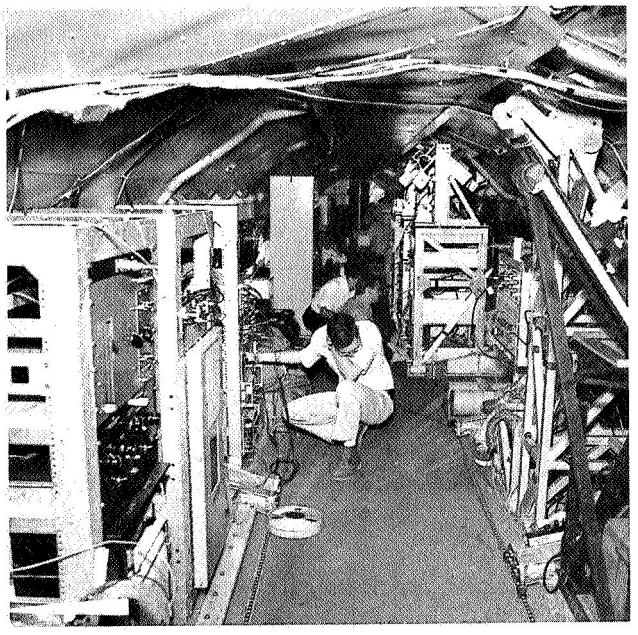

Figure 4—View down the aisle towards the rear of the aircraft.

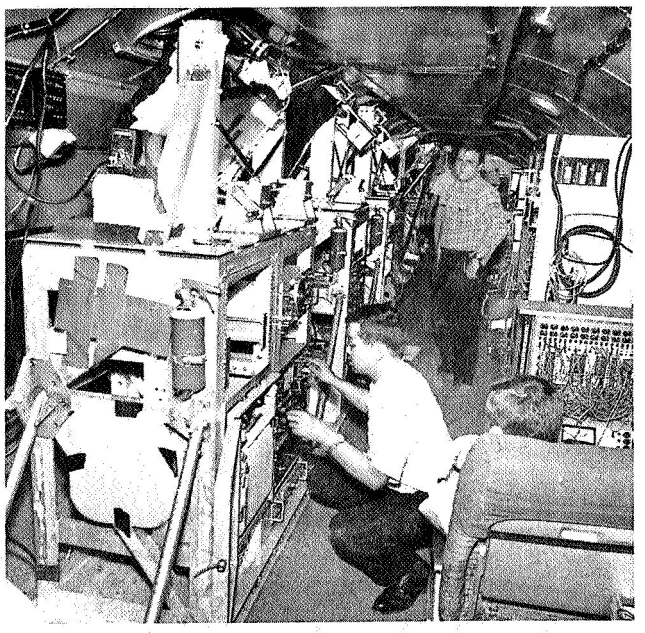

Figure 5—View up the aisle towards the front of the aircraft.

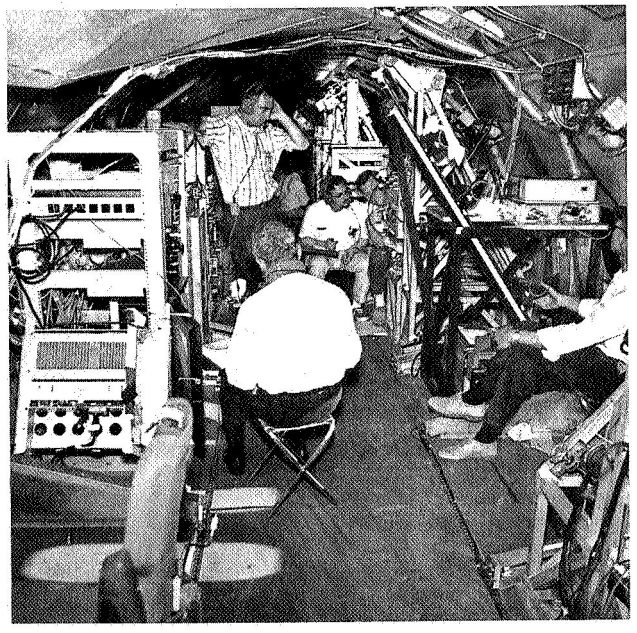

Figure 6—Front section of the aircraft—experimenters during in-flight calibration of the equipment.

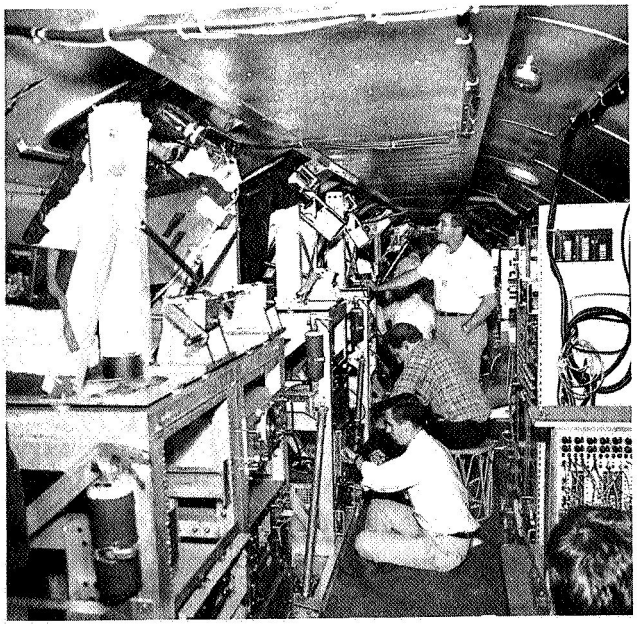

Figure 7—Mid section of the aircraft—experimenters during in-flight calibration of the equipment.

the GSFC Fabrication Division. The construction of the Cary 14 mounts, as also the final modifications required for all the other mounts and racks during the two weeks before the flight, were undertaken by the workshops attached to the Airborne Sciences Office at Ames Research Center.

The design and fixture of the mounts and their arrangement in NASA 711 Galileo can best be shown with the aid of Figures 4 to 7 which are reproductions of photographs taken on board the aircraft. These were taken while the plane was on the ground or in flight on the way to the location.

Figure 4 gives a view from the front of the plane looking down the aisle. Most of the instrument mounts and the racks for the power supply and the electronics can be identified in this picture. On the port side of the plane in front are seen the black-painted slant rails of the Perkin-Elmer. Behind it are the upper and lower mounts for the cone, the mounts for the filter, the E.S.S. and the Leiss. On the starboard side are the control console for the Perkin-Elmer, the tape recorder, the control console for the Hy-Cal and the cone. The experimenters are, front to rear, McNutt, Lester and Park.

Figure 5 which gives a view up the aisle from the rear of the aircraft serves as a complement to Figure 4. The instruments seen on the port side are, front to rear, the Leiss, E.S.S., filter, cone, and Perkin-Elmer. Experimenters are Park and Lester. The pseudo-polar axis mounts of the first three instruments, the handles for tracking the sun and the standard lamp holders can be clearly distinguished in the Figure.

Two close-up pictures of some of the instruments and the experimenters at their respective stations are seen in Figures 6 and 7. Figure 6 shows some of the instruments of the Thermodynamics Branch, the experimenters are left to right—Thekaekara, back to camera, Maichle, Kruger, Ward and Winker. Figure 7 shows the instruments operated by the Thermophysics Branch, the experimenters are, left to right—Webb, Lester and Duncan, standing. These pictures were taken during flight while making calibrations with standard lamps, prior to the solar measurements.

4. THE FLIGHT ALTITUDE AND THE ATMOSPHERE ABOVE THE AIRCRAFT

The flights of NASA 711 for the solar irradiance measurements were made at an altitude of 38,000 feet, except for the first flight of August 3 which was at 38,300 ft. This altitude was chosen as a compromise between minimum amount of atmospheric air above the aircraft and maximum length of observing time. An altitude of 40,000 ft. which had been maintained in the eclipse flights of NASA 711 had first been projected also for the solar irradiance flights. But that would have entailed a sacrifice of about 40 minutes of observing time per flight. The weight of the plane without any load is 118,000 lbs. and that of fuel for 7 hours in air is 85,000 lbs. Compared to these the weight of less than 7000 lbs. for men and equipment is relatively small. The total weight is the major factor which controls the altitude of the flight, thus with 195,000 lbs. the aircraft can fly at 37,000 ft. and with 170,000 lbs. at 39,000 ft. It was decided early in the planning stage that the aircraft would start from Moffett Field with a full load of fuel, fly out to a distant point, thereby expending fuel and bringing the total weight down, make a U-turn and start the data taking portion of the flight. During this portion of the flight the bearing of the aircraft would be normal to the incoming solar rays. The observations would stop at about 15 minutes flying time away from Moffett Field. The higher the altitude chosen for the observation the less would be available fuel and hence

duration of the data taking portion of the flight. The altitude of 38,000 feet proved to be a satisfactory compromise. The altitude is determined from the pressure outside the aircraft as indicated by an aneroid barometer. The conversion from pressure to altitude is made on the assumption of the U. S. standard atmosphere for pressure-altitude variation. Thus, the reading of the aircraft's altimeter represents not so much the exact value of the height above sea level as the weight per unit area of the atmosphere vertically above the aircraft. Since it is the intervening atmosphere which causes the attenuation of the solar energy, maintaining the altimeter at a constant reading ensured the constancy of an important parameter in the solar measurements, the air mass above the aircraft.

The atmospheric pressure at 38,000 ft. is 208 millibars which is 20.5 percent of the pressure at sea level. At 40,000 ft. the pressure is 18.6 percent. The difference though not negligible was considered a small enough tradeoff for the extra observation time which would be available in each flight. A major consideration is that at these high altitudes the atmosphere consists almost entirely of the permanent gases and the relative composition and hence also the attenuation due to Rayleigh and aerosol scattering is independent of geographical location. The factors which contribute most to the uncertainties in ground based measurements, namely, dust, smoke and water vapor become vanishingly small at the high altitudes. Tables of typical moisture content at different altitudes are available in literature[20]; from these data it is seen that the annual average of precipitable water vapor above 38,000 ft. is about 30 microns. It is less than 0.2 percent of the total annual average of precipitable water, 17.9 mm, in the atmosphere above sea level for mean latitudes. An independent measurement was made in September, 1967 by ESSA (Environmental Sciences Service Administration) in the vicinity of Moffett Field from an aircraft at 38,000 ft. From the depth of the main H_2O absorption band at 6 μ, the amount of precipitable water vapor above the aircraft was calculated and found to vary between 12 and 18 microns. Our own findings discussed later show that the H_2O content though varying with date of flight and location was of the same order of magnitude. This is of great significance for measurements of solar spectral irradiance in the wavelength range longer than 7000 A which contains about half the solar energy. The strong predominance of H_2O absorption bands in this range is illustrated in Figure 8, which gives four curves

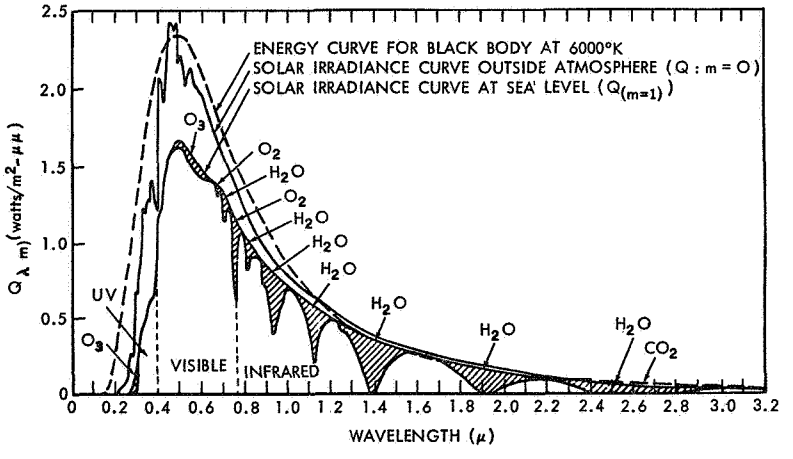

Figure 8—Spectral irradiance curves related to solar energy.

related to solar spectral irradiance. It is reproduced from the section on "Solar Radiation" by Gast[15] in the *Handbook of Geophysics*. The lowest of the four curves with a large number of absorption bands is the solar spectral irradiance as seen from sea level for air mass one, that is, for rays entering the atmosphere normally to the earth's surface. The so-called atmospheric windows are few and narrow, and even in these windows the assumption that the energy is transmitted without any water vapor absorption is open to doubt. For measurements at ground level water is not only a strong absorber but also a highly inconstant absorber. Hence the measurements from a high altitude aircraft can yield a degree of accuracy which is impossible at ground level.

The amount of water vapor within the aircraft is also a factor to be considered. Two independent methods were used. Readings of the wet and dry bulbs of a psychrometer were taken at different locations within the aircraft and on different days. An alternate method was to fill three previously evacuated cans with samples of cabin air and analyze it with a C. E. C. 613 mass spectrometer. Values of relative humidity were between 5 and 10 percent, which correspond to amount of precipitable water vapor per meter of path length between .7 and 1.4 μ. Residual gas analysis of cabin air confirmed this result, the values were .99 μ, .98μ and 1.04 μ respectively for the samples collected during the last three flights. The relative percentages of the permanent gases O_2, N_2 and A were shown by the residual gas analysis to be the same as in normal atmospheric air. CO_2, which in normal air should be only .0314%, was found to be several times higher than expected, namely 16.9, 11.1 and 7.3 times the normal mixing ratio, on the three days. In an attempt to check this anomaly, three other samples of cabin air were taken during later flights of NASA 711 in February 1968. Again the agreement between psychrometric and RGA data was confirmed for water vapor, and CO_2 was found to be 3 to 7 times higher than the normal mixing ratio. It should be noted that this type of residual gas analyzer does not distinguish between CO_2 and N_2O which in normal air is 1/6 percent of CO_2.

The effect of the permanent gases in the atmosphere above the aircraft, though small compared to that at ground level is not negligible, and requires a closer study. Data are available in literature (see Reference 18, pp 7-3 to 7-36) for the extinction optical thickness from height h to ∞ for altitudes at intervals of 1 km for different wavelengths. These are based on Toolin's computations. The transmittance of the atmosphere for any given wavelength is related to the extinction optical thickness by the equation

$$T_{h\infty} = \exp\left(-\tau'_t \sec z\right) \tag{1}$$

where z the zenith angle of the sun, τ'_t is the extinction optical thickness, $T_{h\infty}$ is the ratio of energy transmitted to altitude h to that incident above the atmosphere. τ'_t is the combined effect of Rayleigh scattering, aerosol scattering and ozone absorption. The parameters given by Toolin were computed for U. S. standard atmosphere under certain simplifying assumptions. Table 3 gives the values of τ'_t and $T_{h\infty}$ for sea level and for the altitudes of NASA 711 flights. The values of wavelength are those given by Toolin. Beyond .90μ the six values given are for the optical windows of the atmosphere. The extinction optical coefficients for 38,000 ft. and 38,300 ft. were computed by

Table 3

Extinction Optical Thickness and Attenuation due to the Atmosphere at Sea Level and at the Altitude of NASA 711 Galileo

Wavelength μ	Extinction Optical Thickness from ∞ to h			Attenuation from ∞ to h for normal incidence		
	Sea Level	38,000 ft	38,300 ft	Sea Level	38,000 ft	38,300 ft
.28	37.806	32.618	32.560	3.801×10^{-17}	6.83×10^{-15}	7.24×10^{-15}
.30	4.968	3.110	3.100	6.96×10^{-3}	.0446	.0451
.32	1.551	.4656	.4624	.212	.628	.630
.34	1.046	.1690	.1668	.212	.845	.847
.36	.872	.1179	.1162	.351	.889	.890
.38	.744	.0943	.0929	.476	.910	.911
.40	.619	.0743	.0736	.539	.928	.929
.45	.455	.0479	.0473	.635	.953	.954
.50	.370	.0411	.0406	.691	.960	.960
.55	.331	.0487	.0483	.718	.952	.953
.60	.305	.0553	.0550	.737	.946	.946
.65	.252	.0298	.0297	.777	.972	.972
.70	.217	.0154	.0153	.805	.985	.985
.80	.187	.0084	.0083	.829	.992	.992
.90	.166	.0034	.0034	.847	.997	.997
1.06	.151	.002	.002	.860	.998	.998
1.26	.141	.001	.001	.869	.999	.999
1.67	.126	.001	.001	.882	.999	.999
2.17	.109	0	0	.897	1.0	1.0
3.5	.089	0	0	.915	1.0	1.0
4.0	.080	0	0	.923	1.0	1.0

interpolation from Toolin's values for 11 km (36,090 ft.) and 12 km (39,370 ft.). An important feature revealed by the table of values of transmittance is that at all wavelengths, even in the infrared, there is a considerable difference between the values at sea level and at the altitude of the aircraft. The difference in transmittance for 38,000 ft. and 38,300 ft. is negligible except at .3 μ. For wavelengths less than .3 μ the ozone absorption is so strong that practically no energy reaches the aircraft. The transmittance which is only 4.5 percent at .3 μ increases rapidly to 63 percent at .32 μ and 95 percent at .45 μ. The absorptance of the permanent gases becomes totally negligible only for wavelengths longer than 2μ.

Thus, practically over the whole wavelength range of solar spectral irradiance there is a non-negligible absorption effect due to the atmosphere. The parameters on which these computations are based do not have a sufficient degree of accuracy, nor is the U. S. standard atmosphere exactly valid for the locations of the flight, so that it is necessary to make observations for different zenith angles and to extrapolate to zero air mass using the conventional method of plotting logarithm of the signal versus air mass.

5. THE FLIGHT PATHS FOR SOLAR IRRADIANCE MEASUREMENTS

Six flights were made on board NASA 711 between August 3 and August 19. Summary data on the starting and finishing points of the measurement portion of the flights are given in Table 4. The flight of August 3 was originally intended for checking out the performance of the instruments. All instruments were found to function properly from the very beginning and hence usable data were obtained all through the 2 hours and 10 minutes during which the flight path was normal to the sun's rays. The measurements started at a point which was 1227 miles from Ames Research Center in a direction 14.5° west of south. These values of distance and direction are approximate. The latitude and longitude given in Table 3 were known quite precisely from measurements made on board the aircraft by the navigator. The measurements started at 4:40 p. m. Pacific daylight saving time. The zenith angle of the sun and the air mass given in Table 4 were computed from the known

Table 4

Summary Data on Starting Point and Finishing Point of Measurements on Board NASA 911 Galileo

Flight	Date 1967	Distance to Ames-miles	Direction with Reference to Ames	Time-Hours min PDST	Latitude Degrees N	Longitude Degrees W	Zenith Angle Degrees	Air Mass at 38,000 ft
STARTING POINT								
1. Sunset	Aug 3	1277	14.5° W of S	4:40 pm	19.533	127.167	43.83	1.3858
2. Sunset	Aug 8	1449	20.7 W of S	5:16 pm	17.833	130.000	50.14	1.5596
3. Sunrise	Aug 10	1262	11.3 W of N	7:10 am	55.333	128.500	81.26	6.5290
4. Afternoon	Aug 14	1403	1.3 W of S	2:32 pm	17.133	122.750	18.53	1.0545
5. Mid-day	Aug 16	1297	20.6 N of E	11:06 am	44.000	98.583	31.01	1.1665
6. Afternoon	Aug 19	1413	4.0 W of S	2:31 pm	17.000	123.667	18.01	1.0514
FINISHING POINT								
1. Sunset	Aug 3	135	17.6° S of W	6:50 pm	36.750	124.267	73.15	3.4420
2. Sunset	Aug 8	183	19.8 S of W	7:40 pm	36.333	125.250	83.14	8.2713
3. Sunrise	Aug 10	250	6.4 S of W	9:43 am	37.000	126.717	54.74	1.7313
4. Afternoon	Aug 14	176	13.5 S of W	5:02 pm	36.833	125.250	52.86	1.6555
5. Mid-day	Aug 16	333	20.8 E of N	1:30 pm	41.917	119.883	28.18	1.1406
6. Afternoon	Aug 19	294	34.3 S of W	5:00 pm	35.003	126.500	52.23	1.6319

parameters of latitude, longitude, time and date as will be discussed later. The measurements ended at a point which was 135 miles from Ames in a direction 17.6° south of west and at time 6:50 p.m. Similar data for the flights of the other five days are also given in the table.

The second flight started later in the afternoon and observations were continued until the sun was 6.86° above the horizon. The third was an early morning flight for which the experimenters and crew were in the airplane at 3:30 a.m. As the sun began to rise over the mountains of Canada the plane started to make a U-turn, and the observations started at 7:10 a.m. with the sun at an elevation of 8.74° above the horizon. During these three flights we had the advantage of measuring the solar irradiance over a wide range of zenith angles, 43.83° to 83.14°, the corresponding air masses being 1.386 and 8.271. All the instruments which had mounts designed for use with both upper and lower windows were directed to lower windows. Measurements were made with the other instruments during the portion of the flight when the elevation of the sun was sufficiently high to illumine the integrating sphere from the upper window.

The fourth flight was an early afternoon flight when all 12 instruments could be directed towards the sun during the whole of the data taking portion of the flight. The zenith angle changed from 18.53° to 52.86°. At the start all instruments were turned towards the upper window, but in the course of the flight, Cary 14 and the seven instruments in the front section of the aircraft had to be changed from the upper to the lower window. This was accomplished without any significant loss of time. But another factor which could not have been provided for made this flight break the perfect record of clear skies and usable data which had been established thus far. There was a hurricane over the Pacific Ocean west of Mexico that day and the weather forecasts on which we had relied for the exact location of the hurricane proved to be in error. This is not surprising since our flight was in an area little traveled by commercial aircraft and hence deficient in weather reports. During the first hour of the data taking portion of the flight the aircraft was closer to the eye of the hurricane than had been anticipated and there were large masses of cirrus clouds above the aircraft. Hence we decided to change our original plans for the final flight of the series and to schedule for that day a similar flight path with the same range of solar zenith angle and air mass. We had originally intended for the flight of the final day a series of three elongated ellipses over much the same geographical area south of Ames. This "race track" flight path would have shortened the total observing time but would have served as a check on the variation of atmospheric opacity, if any, over the 1000 or more miles of each of the other flights. However, getting usable data during all of an afternoon flight and from all 17 instruments seemed more important for the whole program than investigating the probably small effect due to the latitude variation of the ozone layer. The increased observing time was another consideration for changing the "race track" plan.

The fifth flight of August 16 was in an east to west direction, with the sun shining from the south. Because of the requirement that the data taking portion of the flight should end near Ames, the flight path was not over the ocean but over western United States, from South Dakota, across the states of Wyoming, Utah and Nevada, and over the Rocky Mountains. Our fears of meeting more cirrus clouds over land than over water proved to have been wrong. In fact this flight gave us the clearest skies, and the least aircraft-roll, so that the signals received by the instruments were quite strong all during the flight.

The final flight of the series for repeating the zenith angle range of August 14 was made on August 19. The flight started from Oakland Civil airport since Moffett Field had been reserved by U. S. Navy for a major annual airshow for the morning. High altitude cirrus clouds again caused a minor change in flight path, but useable data were obtained all during the flight.

During each flight, at intervals of ten minutes, the flight navigator made measurements of the latitude and longitude of the aircraft location. Figure 9 is a map of the geographical area covered in the six flights with curved lines showing the route taken during the data taking portion of each flight. Each flight path is indicated by the date and by the time in Pacific daylight saving time (P.D.S.T.) of start and finish of data acquisition.

The position data provided by the navigator using Loran A and doppler radar are considered accurate to within 10 nautical miles. These data were used in a computer program to calculate the zenith angle of the sun and the air mass above the aircraft at one minute intervals. Air mass data are needed to determine the solar irradiance for zero air mass, that is, in the absence of the earth's atmosphere. Air mass is defined as the ratio of the distance travelled by the rays of the sun in the atmosphere for a given zenith angle of the sun and altitude of observer to the distance for same altitude and zenith angle zero. Air mass is unity when the sun is vertically above the observer. For other positions of the sun air mass is the secant of the zenith angle in the first degree of approximation. The zenith angle may be directly measured by a sextant or may be computed from the known values of latitude, longitude and time. Since the aircraft was a moving platform, it was decided that instantaneous computed values of position over the ground would be more reliable.

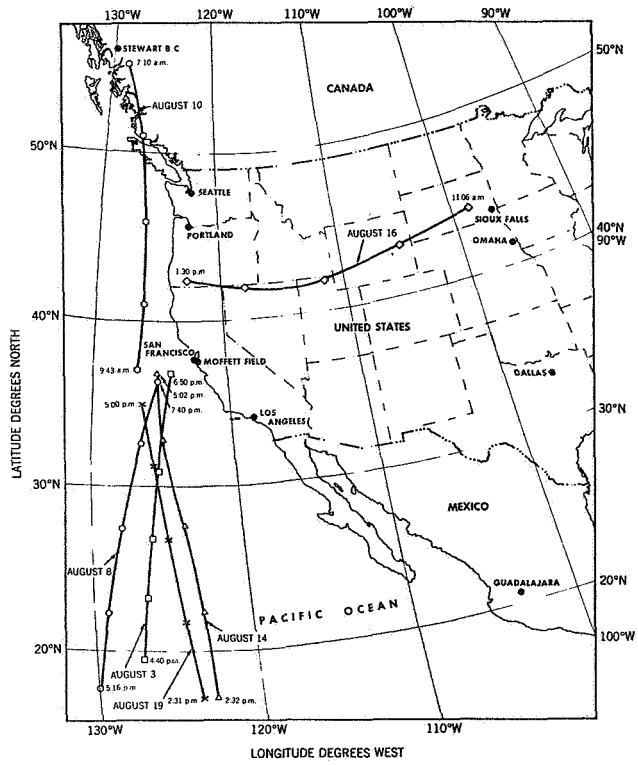

Figure 9—Flight paths of NASA 711, Galileo, solar irradiance experiments, August 1967.

The zenith angle z is related to latitude ϕ, declination of the sun δ and the hour angle of the sun h by the equation

$$\sec z = (\sin\phi \sin\delta + \cos\phi \cos\delta \cos h)^{-1} \quad (2)$$

Basic data for computing δ and h at any given location and time are available in *The American Ephemeris and Nautical Almanac*.[21] Values of δ are given for 0^h G.C.T. (Midnight Greenwich civil time) for every day of the year, from which by linear interpolation δ for time t P.D.S.T. can be found. The hour angle of the sun is 15° times the difference between the time of the day and the

time when the sun crosses the meridian. The time of the day in this case is the local true solar time which is slightly different from the local mean solar time. The difference between the two is the equation of time. The local mean time varies with the longitude, being exactly equal to the Pacific standard time at longitude 120° west, and decreasing by 4 minutes for every degree increase in longitude. The variables, declination at 0^h G.C.T., change in declination per hour and equation of time, for each day of the flight were obtained from the *American Ephemeris and Nautical Almanac*. An expression for zenith angle dependent on these three variables, and the three variables of the flight path, namely, latitude ϕ, longitude θ and time in P.D.S.T., was derived and programmed for the computer. The input data for computing ϕ and θ were the values at 10 minute intervals supplied by the flight navigator. The first three pairs of consecutive values of ϕ and t were fitted to an equation of the second degree to give ϕ for increments of one minute. Then the first pair of ϕ and t was replaced by the 4th pair to extend the interval by 10 minutes. Thus in every interval except the first and last, two values of ϕ are available for a given t; any difference between the two is due to slight deviations from the parabolic path or more likely to rounding off errors in reading the latitude. A similar method was employed for finding θ at one minute intervals.

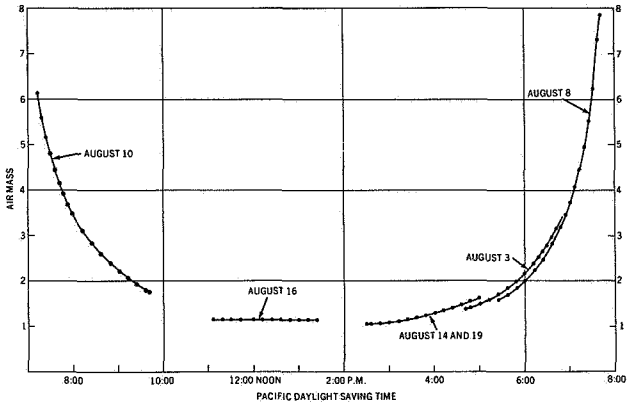

Figure 10—Variation of air mass with time for the flight paths of NASA 711.

Equating the air mass to the secant of the zenith angle is valid only in the first degree of approximation, and does not take into account the decreasing air density in the upper layers of the atmosphere and consequent bending of the sun's ray as it passes from a rarer to a denser layer. Two formulae are available for obtaining a more accurate value of the air mass for ground-based measurements, one due to Bemporad[22] published in 1907 and widely used by many of the early observers of solar irradiance and a more recent one due to Kasten[23] published in 1964. The latter is computed from the air density profile of the U. S. standard model atmosphere proposed in 1959 by the Air Force Research and Development Command, and is considered more accurate. However, for measurements at 38,000 ft, above 80% of the atmosphere, Kasten's formula is over-corrected. The value of air mass at 38,000 feet which we have used as being most satisfactory is a weighted average of secant of the zenith angle and the value given by Kasten's formula, with relative weights in the ratio 4 to 1. Figure 10 shows the variation of air mass with time on the six days of the flight. On August 10 the air mass was practically constant. There was a small change on August 14 and 19. On the other days the change was over a wide range. Early morning on August 10 and late evening on August 8 the air mass changed very rapidly with time.

A sample of the table of aircraft location and air mass which was prepared soon after the flights and distributed to all the experimenters is shown in Table 5. Only 10 minutes of flight time from August 8 are shown here. The first and last entries of the latitude and longitude are from the flight navigator. The rest are by parabolic interpolation. The average zenith angle and the air mass at

Table 5

Air Mass Computation from Location of the Aircraft and Time of Day—
Sample Data for 10 Minutes of Flight Time on August 10, Sunrise Flight.

Time Pacific D.S.T.	Latitude Degrees North	Longitude Degrees West	Zenith angle of the Sun Degrees	Air Mass Bemporad's Formula	Air Mass Kasten's Formula	Average zenith angle from 2 Interpolations	Air Mass at 38,000 ft.
7:20 a.m.	54.383	127.833	79.72	5.4564	5.4395	79.72	5.5705
7:21	54.272	127.778	79.57	5.3833	5.3668	79.575	5.4947
7:22	54.157	127.726	79.42	5.3125	5.2963	79.43	5.4210
7:23	54.039	127.675	79.28	5.2438	5.2281	79.29	5.3516
7:24	53.919	127.627	79.13	5.1773	5.1619	79.14	5.2793
7:25	53.796	127.581	78.98	5.1128	5.0977	78.995	5.2113
7:26	53.669	127.537	78.84	5.0501	5.0354	78.85	5.1450
7:27	53.540	127.495	78.69	4.9893	4.9750	78.70	5.0782
7:28	53.407	127.456	78.55	4.9303	4.9163	78.56	5.0175
7:29	53.272	127.418	78.41	4.8729	4.8592	78.415	4.9561
7:30	53.133	127.383	78.27	4.8171	4.8037	78.27	4.8962

38,000 feet given in the last two columns are based on two sets of interpolations. The final column, as stated earlier is $(0.8 \sec \theta + 0.2\, l_k)$ where l_k is air mass from Kasten's formula.

Another factor which has to be considered as a correction factor common to all the instruments is the distance of the earth from the sun. The solar constant and spectral irradiance are defined for the mean sun earth distance, which is the semimajor axis of the earth's orbit or one astronomical unit (A. U.). During the days of the flight the ratio of the sun earth distance to one A.U. had the following values: August 3: 1.0146, August 8: 1.0139, August 10: 1.0136, August 14: 1.0128, August 16: 1.0125, August 19: 1.0119. These values were obtained by interpolation from those given in U. S. Nautical Almanac for every day at zero hour G.C.T. with due corrections for actual flight time and the difference between G.C.T. and P.D.S.T. It is seen that since the sun was at a distance greater than average during the flight days the values obtained from our observations have to be increased by percentages varying between 2.9 and 2.4 to give the solar constant and spectral irradiance.

PART II

SOLAR TOTAL IRRADIANCE EXPERIMENTS

A. THE CONE RADIOMETER

R. Kruger

1. DESCRIPTION OF EQUIPMENT

The wire wound cone radiometer was one of the instruments used on board NASA 711 for measuring the total solar irradiance. Figure 11 shows all the total radiation detectors, unmounted and placed side by side to indicate their relative size. Left to right are seen, after the limiting diaphragm of the cone radiometer which is to the extreme left, 1) the cone radiometer in its vacuum enclosure, 2) the Ångström pyrheliometer, 3) the Hy-Cal pyrheliometer and 4) the Eppley normal incidence thermopile.

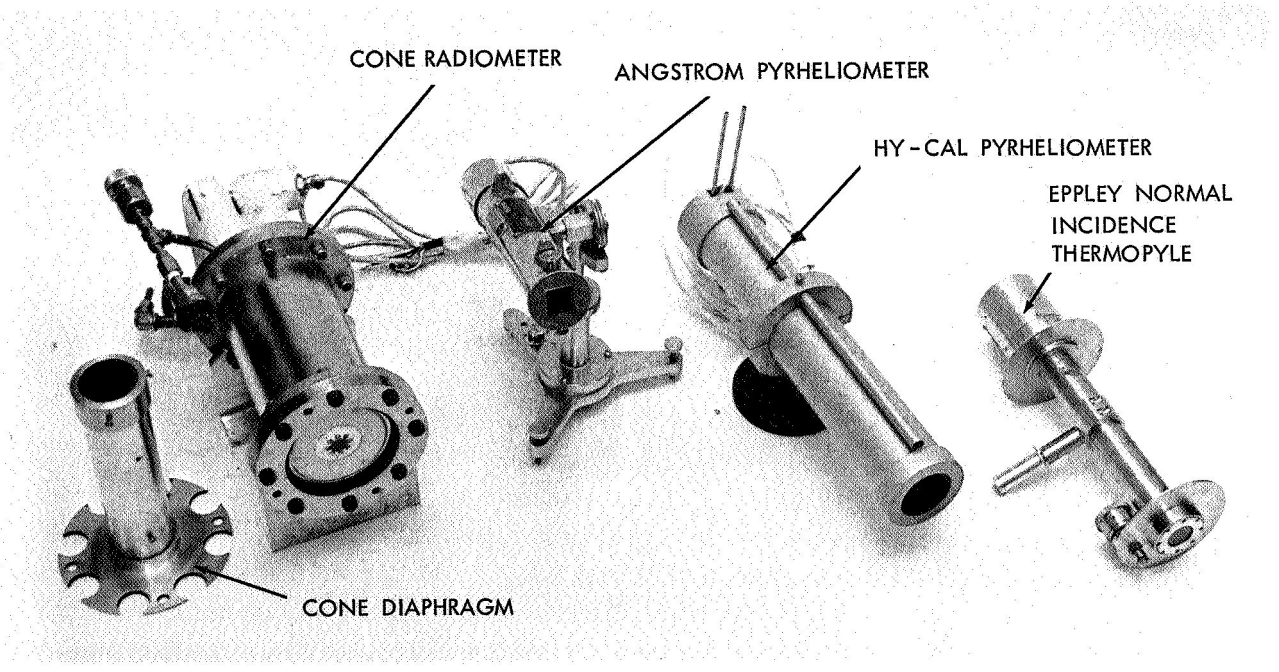

Figure 11—Total radiation detectors.

The cone radiometer is designed to operate as an absolute total radiation detector using an electrical power substitution method. It is therefore referenced to the scale of absolute electrical units. The radiometer is designed to operate in a vacuum environment where gaseous conduction and convection may be neglected.

The theory behind the operation is relatively simple. If an electric current is passed through a wire wrapped in the shape of a cone with the base open, the energy dissipated will be radiated out through the base of the cone and through the slant conical outer surface. If the slant surface is enclosed in a housing whose temperature is maintained constant, the energy incident from this enclosure to the slant surface may be considered constant. The energy incident on the base of the cone is a function of the environment viewed by the base. If, after stable conditions are reached, the energy reaching the base is changed, the wire temperature and resistance will change. If these are returned to their original values by varying the current through the wire, the change in electrical power is then a measure of the net change in the radiant energy falling on the base of the cone.

The detector used in this program was made by wrapping a fine wire (0.002 inch diameter insulated nickel wire) on a 30° apex angle conical mandrel. The wire was then thinly coated with an aluminum filled epoxy, removed from the mandrel, and painted inside and out with Parsons' black matte lacquer. The unit had a mean base diameter of 9.65 mm. The effective absorptance of the detector was taken as 0.9945 based on the work of Gouffé.[24] This value is open to question but is, however, used in this paper. A value of 0.99 for a cone would result from the method of Campanero and Ricolfi.[25] The actual value of the area times the absorptance used in this report is 0.7364 which includes corrections for the area of the rim of the cone and its absorptance (0.9) and a 1.9% correction which will be discussed later. If the value of 0.99 is chosen for the conical absorptance and .96 for rim absorptance, the area times absorptance is less than .1% different than the value used for this report.

The detector is mounted by fine wires at four points inside a housing or block which is cooled by liquid nitrogen. The block is made of copper to improve isothermality. Figure 12 is a drawing of the radiometer configuration. The block is shaped so as to prevent reflection from the front surface into the detector. The interior is conically shaped to decrease to a negligible amount that light which passes through the annulus between the detector and the front of the block and is reflected onto the slant surface of the cone. The interior of the cavity is coated with 3M Velvet flat black paint.

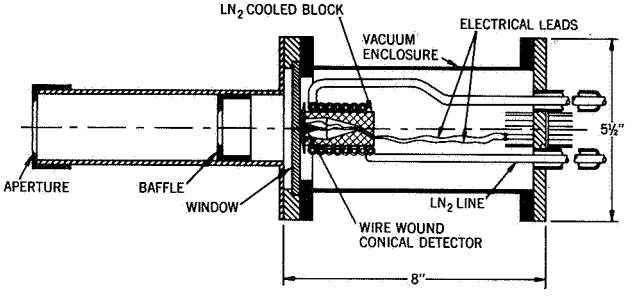

Figure 12—Drawing of cone radiometer

The block and detector are enclosed in a vacuum tight chamber which has a sapphire window. This material was chosen for the window because of its mechanical and optical transmission characteristics (no absorption bands from .2 to 6 microns). The chamber itself is constructed of stainless steel with Viton o-rings used on the sealing surfaces and teflon used for both thermal and electrical insulation.

The aperture system is designed in accordance with the method of A. Ångström.[26] Two acceptance angle apertures were manufactured, one with approximately a 3° acceptance angle

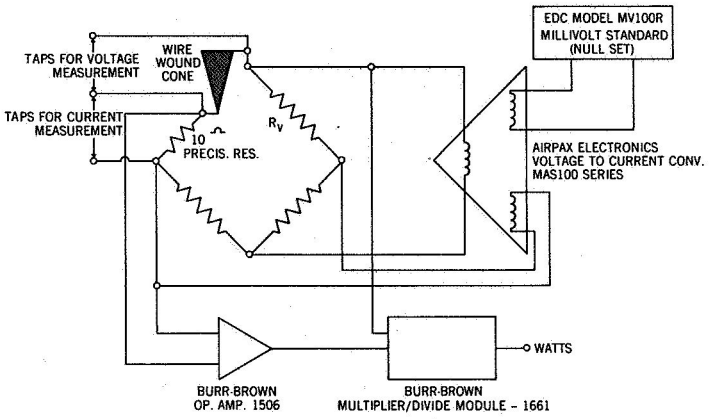

Figure 13—Electrical diagram of cone radiometer.

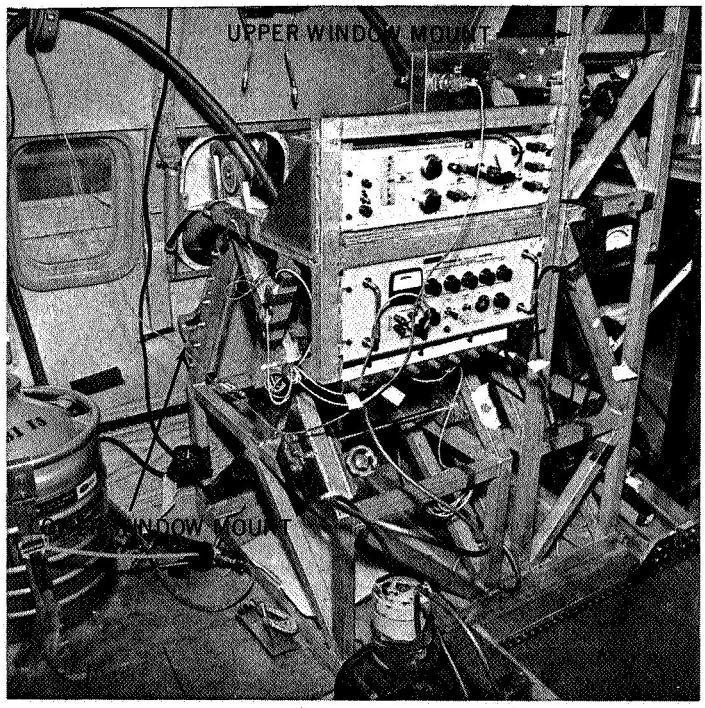

Figure 14—Cone radiometer mounting.

and a second giving an angle of $5\frac{1}{2}°$. The $5\frac{1}{2}°$ aperture was used for most of the flight. The other unit was used for a short period during the test but no difference was detected.

Figure 13 is a schematic representation of the electrical system. The conical detector forms one leg of the Wheatstone bridge. Resistor R_v is varied according to the energy level to be detected. For this series of tests, the cone resistance was about 206 ohms which happens to correspond to a temperature of 23°C. A voltage to current converter provides the bridge voltage and detects the null. Changes off null are sensed by the converter and the bridge voltage is varied to return the system to null.

The data for this report was hand recorded. A Dana digital voltmeter, model 5600, was used to measure the voltage across the cone and across the 10 ohm precision resistor to determine current. Data was also recorded from the Burr-Brown multiplier/divider unit, model 1661, which yields a direct measurement of electrical power by supplying the product of voltage and current.

The mounts for the cone radiometer are shown in Figure 14. The control panels for the electrical circuitry were attached to the lower window mount.

2. EXPERIMENT PROCEDURE

Prior to each flight, the electrical system was checked to assure that it was operating. The liquid nitrogen dewar and pressurization system were filled. A mechanical pump was used to evacuate the radiometer housing; this would normally bring the unit to the order of 15 microns pressure. The system was then valved shut and liquid nitrogen fed to the cooled block. This caused a further reduction of pressure by cryopumping to a final value ranging between 0.7 and 2.8 microns pressure as measured by a Hastings thermocouple gage. Although this is not

sufficient vacuum to eliminate gaseous conduction and convection, these terms are reduced to where they are small and nearly constant. The use of the zero readings provides a method for decreasing the effects of pressure variations.

On the flight out to the data taking leg, liquid nitrogen flow was stabilized and the block operated during the tests at -185°C ± 2°. The electronics were given one to two hours to warm up.

During the data taking leg, the system was checked for null and hand recordings were made of time, voltage and current through the cone, off-null current, bridge voltage, millivolt standard output, block temperature, and chamber pressure. The latter four values were only checked occasionally to assure that no gross changes occurred. Data from the Burr-Brown model 1661 were recorded on the Ampex CP-100 tape recorder; time, synchronized with WWV, was also recorded on the magnetic tape. The output of the Burr-Brown model 1661 was corrected several times each flight to equal the power as calculated from the digital voltmeter readings.

During the flight, tracking was manually accomplished as explained in Part I of this report. Aside from occasional large excursions due to aircraft motions, the system could normally be kept aligned to within $\frac{1}{2}°$ of angle.

3. DATA ANALYSIS

a. Data Selection

The data for this report is taken entirely from the hand recorded data. While the tape recorded data was accurate to within 1%, the multiplier/divider unit was found to be in error by 2% on some occasions when corrections were being made. The tape recorded data did provide information of a qualitative nature in particular as to whether the electronic system was stable; also, the voice channel was used as a log.

Of the hand recorded data, some have been discarded for various reasons. 25 readings were omitted when a review of the data showed a marked shift and increase in scatter for these points. This happened on the two days when the instrument was moved from the upper to the lower window; the erratic data occurred when the detector was moved to the lower window. A careful layout of the equipment indicated a high probability that light could be scattered off the window aperture edge and into the detector. 20 readings were eliminated when log notations indicated light haze and other atmospheric disturbances. Other data were discarded for reasons such as cone resistance outside an error limit, electrical system being unstable, and a question of whether the radiometer window was parallel to the aircraft window. This last item is very angle sensitive and would cause an increase in transmittance of over 1%.

b. Zero Readings

In order to obtain a best estimate of the net power change in the detector, the zero readings were plotted and a smooth curve drawn through them. The particular value of the zero reading curve at the time of the solar observation was then used as the tare power value.

c. Value of the Solar Constant

The data are presented in Figure 15 which is plotted in the usual manner of a graph of $\log_{10} P$, where P is the total irradiance, versus air mass. The derivation of the air mass is presented in Part I of this report. Corrections for distance to the sun have been applied.

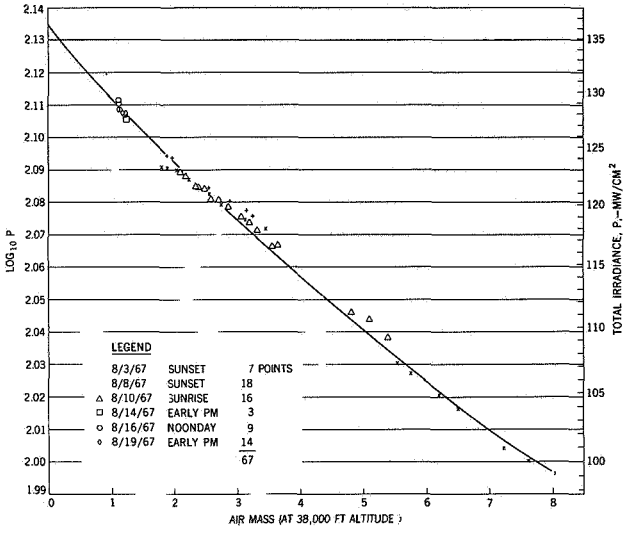

Figure 15—Data from the cone radiometer.

Transmittance of the windows was computed theoretically from the index of refraction adjusted by experimental data in the absorption bands. Variation of transmittance with angle was also computed. Both were compared to laboratory tests and found to be within 0.5%.

The method of extrapolation to zero air mass used herein is believed more valid than passing a least squares fit straight line through the data points. Basically, the curve passed through the points was of the form

$$\log_{10} P = \log_{10} \sum_{i=1}^{n} F_i \tau_i A_i^l \qquad (3)$$

where:

P = total irradiance, mw cm^{-2}

i = an interval of bandwidth of the solar spectrum

F = fraction of the solar energy in interval i

τ = transmittance of optical element in the interval i

A = atmospheric attenuation in the interval i

l = air mass

For this analysis, twenty intervals were used. The result of using this form is a concave up curve which was plotted on transparent paper and slid over the data points until a visual best fit was obtained. A better fit might be obtained by more elegant mathematical means but it was not felt necessary. The Y-intercept of the curve is then the logarithm of the solar constant.

Since a family of curves may be built up by varying the value of "A" in any interval, it was decided to vary "A" in the interval between 1.2 and 1.6 microns in order to obtain a curve which best passed through all the data. Using this approach, a value of 136.4 mw cm^{-2} was found as the value of P, the total irradiance.

A second approach was used which took advantage of the other available data. In this technique, the value of "A" was varied in those three intervals containg the 1.4, 1.9, and 2.7 water absorption

bands. The data from the Perkin-Elmer monochromator in those bands was reviewed for five periods, three on August 10, 1967, one on August 14, 1967, and one on August 16, 1967. The values were 131.9, 134.0, 133.8, 135.6, and 136.0 mw cm^{-2} respectively. It is of interest to note that the readings are arranged in order of decreasing air mass going, in order, 5, 3.6, 2.25, 2.13, and 1.13 and also increasing amounts of percipitable water going, in order, 9, 12, 18, 22, and 28 microns.

d. Sources of Error

The following is a tabulation of sources of error and an estimate of their magnitude; the values are referred to the value of P, the total irradiance.

1.0% — Uncertainty in window transmission

1.0 — Value of "A" used in extrapolation

0.2 — Effect of error in time of day of measurement on air mass; varies from 0.7 at air mass 8 to less than 0.1 at air mass 1.5. The value 0.2 was chosen as including most data.

0.1 — Position over the ground as determined by Loran A and doppler radar.

0.8 — Zero reading shift due to pressure rise while taking a reading; derived from laboratory tests.

0.5 — Area times cone absorptance

0.5 — Precision derived from laboratory tests applying inverse square relationship to energy sources.

0.5 — Light reflected from front face of cooled block back to aperture tube and thence to detector; analytically derived but could not be measured in the laboratory

0.1 — Error in measurement; digital voltmeter checked at Ames Research Center to be within 0.01%.

A number of other sources of error exist which are less than 0.1% and have been neglected. These include the effect of being off-null and the effect of light passing through the annulus between the cone and the cooled block. The latter was shown analytically to cause an error in the order of 0.02%.

Applying the method of the square root of the sum of the squares, one arrives at an overall error in the order of 1.8%.

One error which has been corrected for was a bias of 1.9% due to the existance of a slightly rounded edge on the front face of the cooled block. This reflected light into the detector and was noticed during laboratory tests after the flight. The 1.9% figure was arrived at by conducting laboratory tests with the shiny edge painted black.

inch length, which has a quartz window. The spectral range of the window is .2-3.5μ. The output from the detector is a dc millivolt signal which varies linearly with incident irradiance up to 2 solar constants. A calibration curve of millivolt output versus incident radiation is supplied with the pyrheliometer. The pyrheliometer was calibrated by Hy-Cal Engineering by comparison to a standard pyrheliometer calibrated with reference to a blackbody cavity.

2. EXPERIMENTAL PROCEDURE

The Hy-Cal was mounted on the same stand as the Ångström 6618. Figure 16 shows to the left the mounting rack for the detectors (the rear of the Hy-Cal is clearly seen) and to the right the rack for the power supply and galvanometer for the Ångström. The output of the Hy-Cal pyrheliometer was monitored in two ways. First it was read directly from the instrument using a Dana digital voltmeter, model 5600, about 3 or 4 times during each flight. The rest of the time it was amplified by an operational amplifier and recorded on one of the channels of the Ampex CP-100 tape recorder. The time, synchronized to WWV, was recorded on another channel of the same tape, so that a continuous record of signal versus time was available.

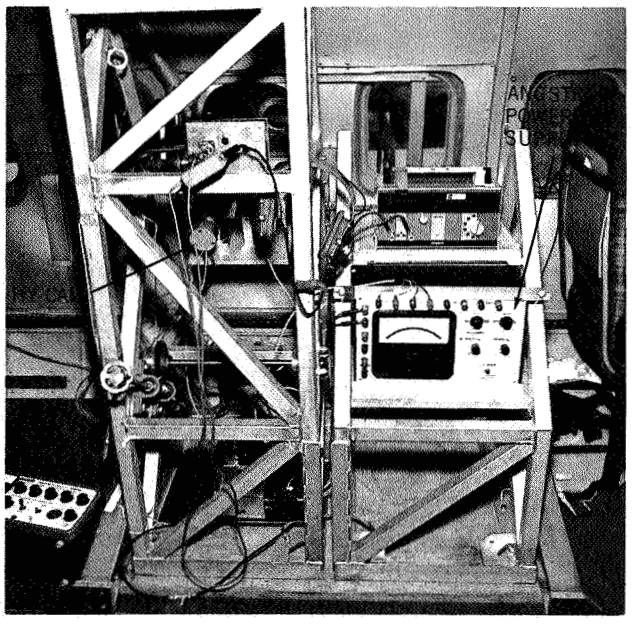

Figure 16—Mounting of the Ångström and Hy-Cal pyrheliometers.

3. DATA ANALYSIS

The Hy-Cal pyrheliometer irradiance values were calculated using the formula:

$$I = 27\ 36\ V \tag{4}$$

where

V = signal in millivolts

27.36 = calibration constant

I = irradiance in mw cm^{-2}

The analog flight tapes were sampled 5 times a second by a computer and averaged over a ten second period. The ten second averages were printed out giving a table of signal in millivolts versus time at ten second intervals. The analog flight tapes were also played into a stripchart

recorder giving a continuous graph of the analog signal as a function of time. The stripchart was used to select periods of time when the instrument was not sighted on the sun or the signal was erratic for other reasons. The ten second averages during these times were omitted. A total of 170 irradiance values were obtained this way. The values obtained from the computer printout agree with the values taken at the corresponding time on the plane with the Dana digital voltmeter to within ±0.5%. The 170 irradiance values were plotted as a function of time and showed a scatter of ±1.0%. The irradiance values were then corrected for window transmission and the mean distance of the earth from the sun in the same way corrections were made for the Ångström pyrheliometer. The $\log_{10}$ of the corrected irradiance values were plotted as a function of the air mass. (See Figure 17). Theoretical curves were fitted to the data as discussed earlier in the section on the cone radiometer.

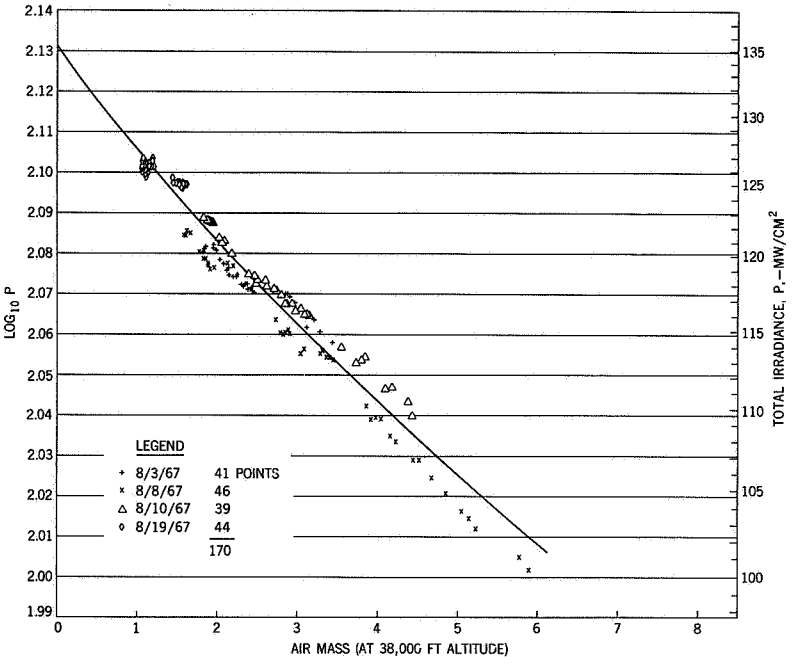

Figure 17—Data from the Hy-Cal pyrheliometer.

4. RESULTS

The data are presented in Figure 17. The intercept for zero air mass is 2.131 which corresponds to 135.2 mw cm^{-2}. The error is 1.6% or ±2.2 mw cm^{-2}.

C. ÅNGSTRÖM COMPENSATION PYRHELIOMETER 6618

A. McNutt and T. A. Riley

1. DESCRIPTION OF EQUIPMENT

Another of the total radiation detectors was an Ångström Compensation Pyrheliometer 6618. It consists of two ribbon detecting surfaces located at the rear of a tube, 9 inches long and 2 inches in diameter, containing rectangular apertures and a shutter. The shutter allows the left or right or both ribbons to be exposed to the incident radiation. The ribbon is located at about 5" behind the front of the instrument. The front aperture is such that each ribbon has plane angles of 4.2° and 10.6° as measured from the center of the ribbon to the edges of the aperture which admits radiation to it. The detector ribbons are manganin sprayed with Parsons' matte black optical lacquer. Each strip has a copper-constantan thermocouple in thermal but not electrical contact with it and can be heated electrically by passing current through it. Measurements are made by exposing the left ribbon to the incident radiation and heating the right ribbon electrically until both are the same temperature. The current necessary to heat the ribbon is measured. The shutter position is then changed so that the right ribbon is exposed and the left is electrically heated and the current is again measured. The average of the two measured currents and a calibration constant gives the value of the incident radiation. The calibration constant is furnished with the instrument and is determined by comparison to a standard pyrheliometer. The auxiliary equipment consists of a Kipp and Zonen galvanometer, model AL-1, which indicates when the ribbons are at the same temperature and a battery power supply and meter for measuring the current. They were mounted on a separate stand, as shown to the right in Figure 16.

2. EXPERIMENTAL PROCEDURE

A measurement was made about every 2 to 4 minutes during a flight and took about 1 minute to get both a left and right ribbon exposure. The time of measurement was accurate to the nearest minute. The time and the current measurements were recorded by hand.

3. DATA ANALYSIS

The irradiance values measured by the Ångström pyrheliometer were calculated using:

$$P = Ka^2 \tag{5}$$

where P = irradiance in mw cm^{-2}

K = calibration constant

a = average of left and right currents.

The calibration constant K was checked by A. J. Drummond of Eppley Laboratory at Table Mountain California on August 25, 26 after the series of flights, and was found to be 6.08, a 1.0% change from the original value of 6.02. The value K = 6.08 was used in the reduction of the flight data. The current was measured with an accuracy of ±0.5%, but a plot of irradiance versus time showed a scatter of ±1.5%, so the accuracy of the raw data was assumed to be about ±1.5%. The irradiance values were corrected for transmission of the aircraft window and the mean distance of the earth from the sun. One correction factor for the mean distance was used per flight for each of the six flights. One value for the window transmission was used for all flights and all angles of incidence for both upper and lower windows. This was done since the transmittance changed only 0.5% over the full range of angles of incidence. The method for obtaining the window transmission is described in the cone radiometer data analysis section of this report. The values of $\log_{10}$ of the irradiance were plotted as a function of the air mass. The result is shown in Figure 18.

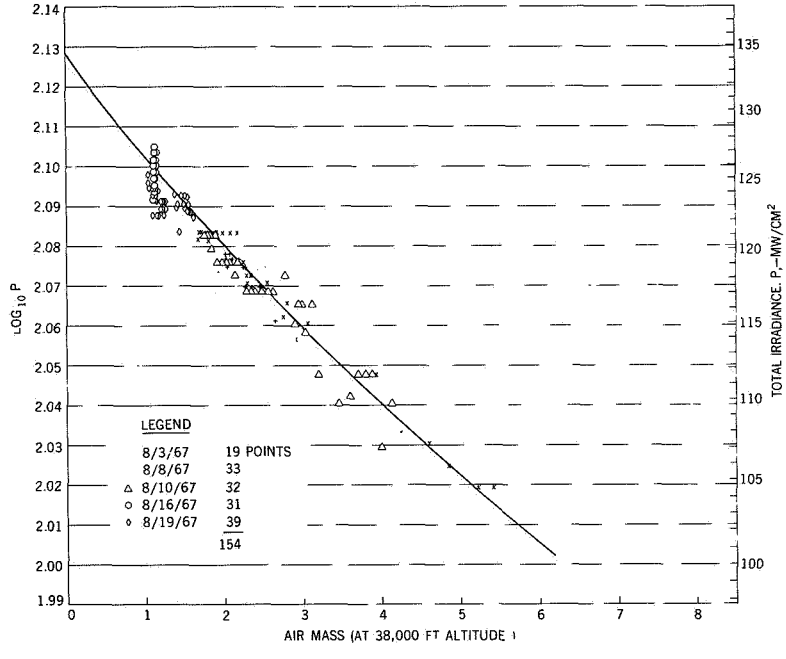

Figure 18—Data from the Ångström No. 6618.

Instead of fitting a straight line to the data by the method of least squares, a family of theoretical curves were generated to see which best fit the data as described in the cone radiometer data analysis section of this report. The uncertainty in the time and position of the plane which affect the air mass value are negligible compared to the uncertainty in the irradiance values. The uncertainty in the window transmittance is of the order of ±1.0%. There is an uncertainty in choosing which curve and where to fit it. This uncertainty amounts to 2.8% for the value for zero air mass.

4. RESULTS

The best fitting curve is shown in Figure 18. The intercept for zero air mass is 2.128 which corresponds to 134.3 mw/cm^{-2}. The error is 1.9% or ± 2.6 mw cm^{-2}.

A third total radiation detector also operated by the Thermodynamics Branch was an Eppley Laboratory manufactured normal incidence radiometer. It was used in place of the Hy-Cal for the first hour of the August 16 flight. It is an apertured instrument with a quartz window. The output is a dc millivolt signal from a thermocouple. A total of four readings were taken using the Dana digital voltmeter. The irradiance is calculated by multiplying the millivolt signal by a calibration factor. The four irradiance values were compared to the irradiance values of the Ångström at the same time. They averaged 1.9% lower. No check was made however on the calibration of this instrument since it was used for such a small portion of the total flight time.

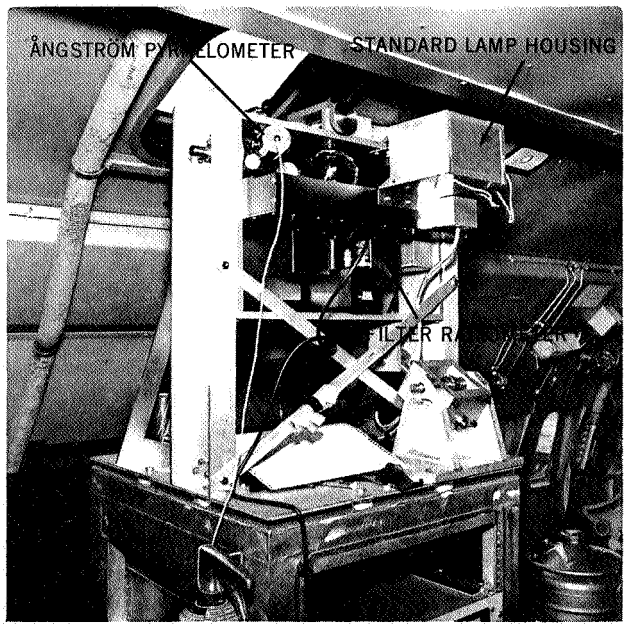

Figure 19—Mounting of the filter radiometer and Ångström 7635.

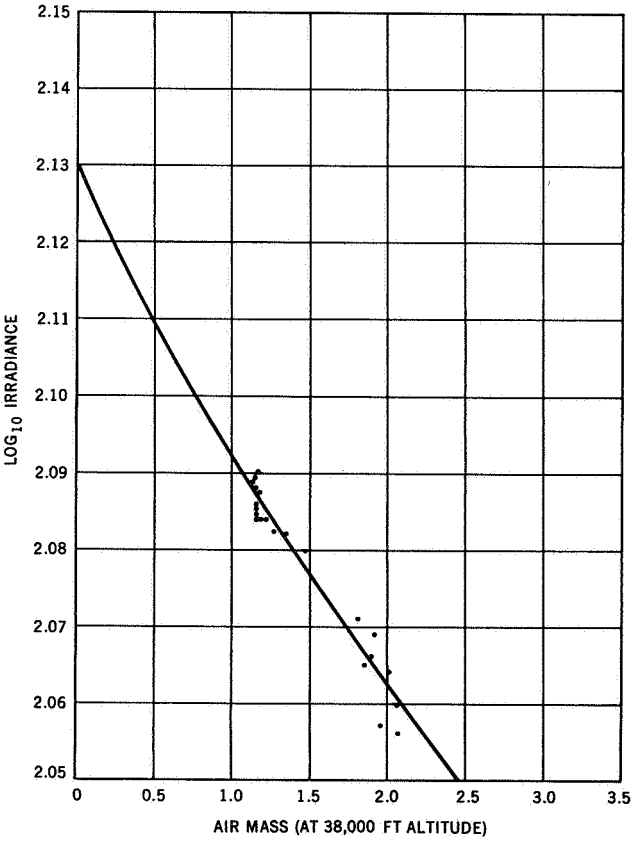

Figure 20—Data from the Ångström No. 7635.

D. ÅNGSTRÖM COMPENSATION PYRHELIOMETER 7635

C. H. Duncan and J. J. Webb

1. DESCRIPTION OF THE EQUIPMENT

A description of this type of instrument is given under the preceding section of this report concerning Ångström 6618. This unit was originally not among the planned instrumentation. It was adapted to mount on the filter radiometer frame after the first flight and data were recorded for the remaining flights. The pyrheliometer can be seen in the photograph in Figure 19.

2. DATA ANALYSIS

After the flight program, Ångström 7635 was calibrated both at Table Mountain and later at the Eppley Laboratories. The instrument was not stable during the two days at Table Mountain and A. J. Drummond of Eppley, who was present during the calibration measurements, recommended an average value of 6.17 be used for the calibration factor.

A total of 42 measurements were made during the five flights but the readings of August 14 were discarded because of intermittent cloud conditions. The remaining data were corrected and the data were analyzed in the same way as for the other total radiation instruments.

3. RESULTS

The distribution of the data points is shown in Figure 20. The resulting value of total irradiance was 134.9 mw cm^{-2}, which is in good agreement with the other Ångström. The errors in the system (particularly in view of the calibration) are on the order of 3% or ± 4.0 mw cm^{-2}.

PART III

SOLAR SPECTRAL IRRADIANCE EXPERIMENTS

A. PERKIN-ELMER MONOCHROMATOR

M. P. Thekaekara, R. Stair, A. R. Winker

1. DESCRIPTION OF THE EQUIPMENT

A Perkin-Elmer monochromator model 112, with a sapphire window for the aircraft and a lithium fluoride prism as the dispersing element, was one of the instruments used on board NASA 711 to measure the spectral irradiance of the sun. Figure 21 shows an optical schematic of the instrument. Light from a diffusing mirror enters the instrument through an adjustable slit and is rendered parallel by a paraboloid mirror. A system of plane mirrors causes the beam to traverse the prism four times, thereby increasing fourfold the resolution obtainable from a single prism. After traversing through the prism the beam is focused either on a thermocouple or on an exit slit behind which is mounted a photomultiplier tube. Scanning the spectrum is done by a littrow mirror located behind the prism; the wavelength falling on the detector is indicated by the count on the drum which controls the rotation of the mirror.

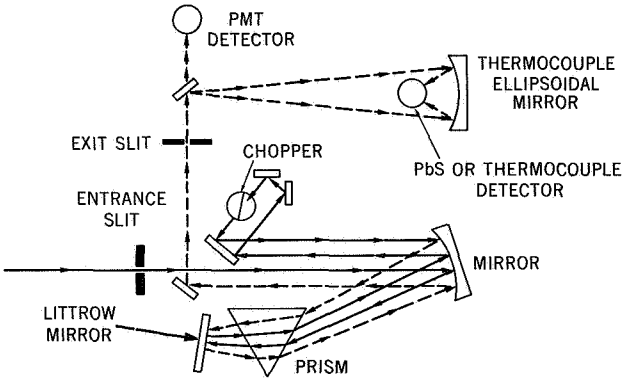

Figure 21—Perkin-Elmer monochromator, optical schematic.

An electronic console carries the amplifiers for the detectors, high voltage supply for the PM tube, a strip chart recorder, step-switch for gain setting of the amplifier and speed control of the littrow mirror, and several other features which make the Perkin-Elmer a highly versatile and automated instrument. A few modifications were introduced to make the instrument more suitable for the solar irradiance measurements. A helical potentiometer with a voltage divider was attached to the drum in order to generate a voltage which changed linearly with the drum count. Another voltage divider was connected to the gain control switch to generate a step voltage which changed by pre-set increments as the gain setting was increased. The output signals from both these as also from the detector amplifier circuit were recorded on three of the channels of a tape recorder. A block diagram of the detection amplification system is shown in Figure 22. Modifications introduced at GSFC for recording the data on magnetic tape are enclosed in heavy lines.

The Perkin-Elmer was mounted on the plywood top of a rigid frame as shown in Figure 23. Sunlight falls on a diffuse mirror which is in front of the slit. The diffuse mirror was prepared

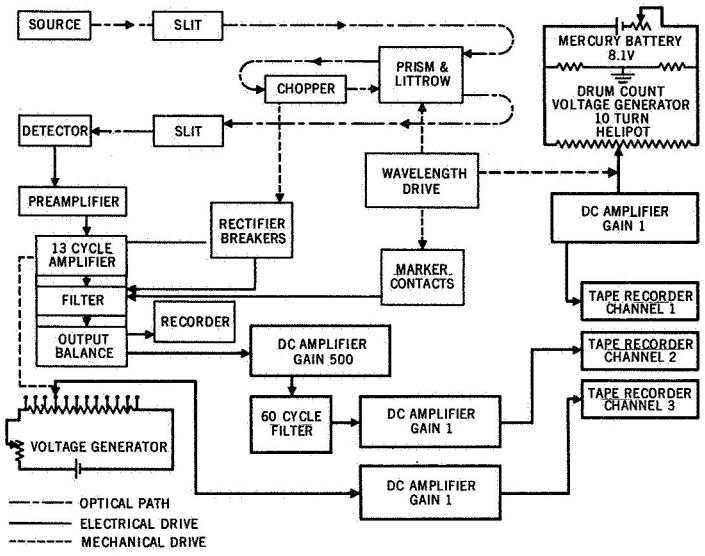

Figure 22—Block diagram of Perkin-Elmer data system.

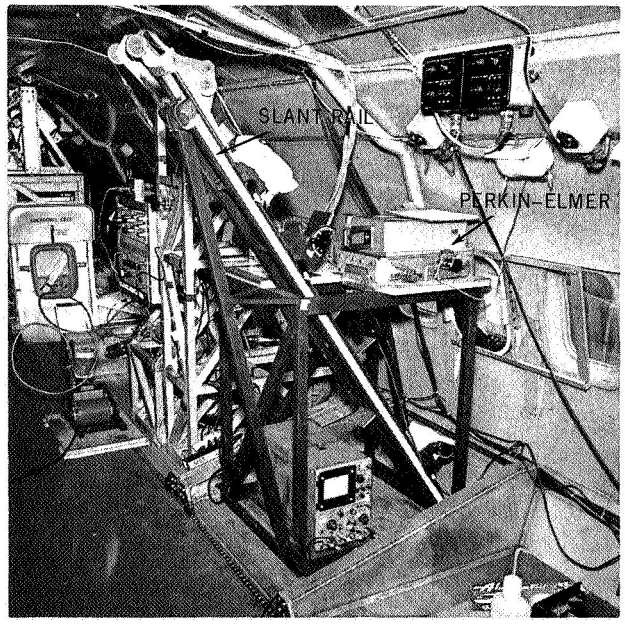

Figure 23—Mounting of the Perkin-Elmer monochromator.

at GSFC by evaporating aluminum on a ground glass surface. Tests had previously been made on two other types of diffusing surfaces, magnesium carbonate block which many observers have used in previous solar irradiance measurements[16], and gold evaporated on frosted glass. Aluminum was found to have a higher reflectance over the whole wavelength range of the LiF prism. Some type of diffusing surface is essential for the solar measurements since the conventional method in spectroscopy of focusing the source on the entrance slit would have limited the observation to a very narrow strip on the solar disc and our interest is in the irradiance due to the whole disc. A plane diffuser was preferred to the integrating sphere because it increases the energy about ten-fold;[27] in the wavelength range 2 to 4μ where solar energy is quite weak, low signal to noise ratio would have made the integrating sphere wholly unacceptable. The diffusing mirror is not, however, illuminated in the same manner by the collimated light of the sun and the divergent beam from the quartz-iodine standard lamp. The standard lamp illumines the whole mirror, whereas the sun, shining through the 4" window of the airplane, illumines a limited elliptical area on the mirror and this area shifts a little with the pitch and roll of the plane. Hence a rectangular diaphragm of adjustable area was mounted a short distance in front of the entrance slit. Maximum area of diaphragm was used only for portions of the flight which were free of all

turbulence. Sunlight was reflected to the diffusing mirror by one of two plane mirrors mounted on a pair of slant rails which also carried the diffuse mirror. The three mirrors with their dust cover on can be readily identified in Figure 23. The height as also the angle of the plane mirror was adjusted during the flight, and the upper or lower mirror was used according to the position of the sun in the sky. The diffuse mirror was fixed in height and its angle had one of two possible values according to the aircraft window which viewed the sun.

2. EXPERIMENTAL PROCEDURE

During the six flights of NASA 711 Galileo, a total of 71 spectral scans of the sun were made. Barring a few exceptions all the scans followed the same uniform procedure. The range of drum count was 2000 to 1100, wavelength .2945μ to 2.53μ, except during the mid-day flight of August 16 when the sun shining through the upper window permitted the range up to 600 drum counts, 3.884μ, to be scanned. Each scan started with the PM tube as detector, slit width 0.1 mm, drum setting a few counts more than 2000. At count 2000 the drum voltage was turned on. At count 1550, wavelength .63μ, the wavelength scan was stopped, slit-width changed to 2 mm, detector changed to thermocouple, and the scan was continued. At the end of the scan, the drum voltage was turned off, and height and angle of the plane mirror was readjusted to begin the next scan. The changeover from PM tube to thermocouple and from one scan to the next could be made in less than 30 seconds, so that spectral scans were made almost continuously from the time the aircraft completed the U-turn to view the sun till it turned off the sun to start the descent to Ames. Scanning speed was 100 counts per minute, so that each scan was made in a little over 9 minutes. The scans of August 14 took 14 minutes each. The chart speed which was 1.25" on August 3 was increased to 5" per minute for the five later flights.

Figure 24 shows a typical strip chart record in the PM tube range. It is a tracing based mainly on the scan made from 12:28 to 12:33 pm on August 16. Short sections from two other scans have been added to complete the record at the changes in gain setting. All the spectral scans are quite similar to the one shown here, except that the pen displacement is less for the lower position of the mirror and for the larger values of the air mass. The effect of the ozone becomes especially noticeable in the range 2950 to 3050 Å for large air mass. The curved lines showing intensity in watts cm^{-2} μ^{-1} have been superposed on the strip chart record.

The calibration with reference to the standard lamp was made several times during flight when the aircraft was going towards the location and in the hangar. The calibration scans made in the aircraft were subject to a small error due to light from the roof of the aircraft. This error was corrected later by comparison with scans made at GSFC. The transfer function of the instrument was highly constant in the photomultiplier range, but in the thermocouple range small fluctuations had apparently occurred due to a misalignment in the instrument.

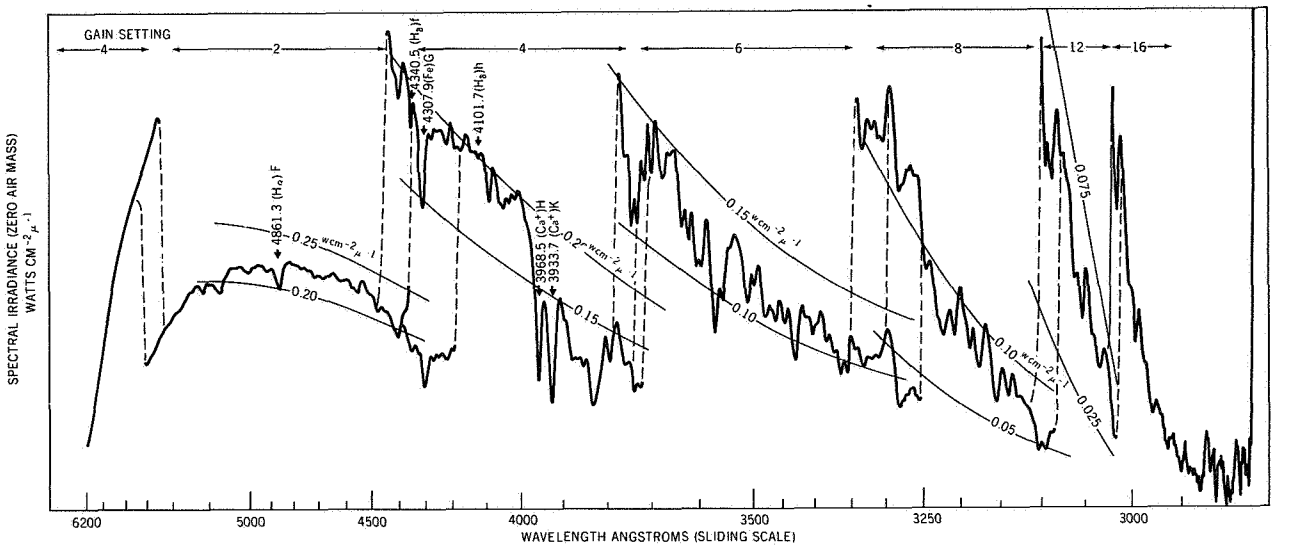

Figure 24—Perkin-Elmer strip chart in the photomultiplier range.

3. DATA ANALYSIS AND RESULTS

The conventional method of determining irradiance from spectrum charts is to compare the chart of the unknown source with that of a standard of spectral irradiance. If the external optics are the same for both charts, the detector output at any given wavelength is proportional to the irradiance, and the following basic equation can be applied.

$$P_x = \frac{A_x G_x}{A_s G_s} P_s \quad , \tag{6}$$

where the subscripts x and s refer to the unknown source and standard source respectively, P is the spectral irradiance, A is the amplitude (deflection of the pen or signal on the tape) and G is a multiplication factor to convert amplitude at a given setting to that at a standard gain setting of 20.

Equation (6) is valid only if the measurements of the sun and of the standard lamps are made under the same conditions, with the same external optics, and that is not the case on board the aircraft. The standard lamp shines directly on the diffuse mirror. The sunlight undergoes attenuation by passing through the atmosphere above the aircraft and through the sapphire window of the aircraft and by being reflected by the specular mirror. Hence, a correction factor is necessary to determine what the signal A_x would be in the absence of such attenuation. Thus, A_x in Equation (6) has to be replaced by $A_x F$, where F is the correction factor. F is the product of three factors, F_a for the atmosphere, F_w for the sapphire window and F_m for the aluminum mirror. $F_a = A^{-1}$, where A is the ratio of solar spectral irradiance at 38,000 feet for air mass unity to that above at the atmosphere, and l is the average air mass during the measurement scan. $F_w = N^2 + 1/2N$ where N is the refractive index of sapphire. F_a is a rather complicated function which we shall not write

down in full here since it is available in standard literature.[28] It is dependent on n and k, the real and imaginary parts of the complex index of refraction, $n + ik$, of aluminum and on the angle of incidence ϕ of sunlight on the specular mirror. The parameters A, N, n and k are dependent on wavelength, but are the same for all solar scans; the parameters p and ϕ change from one scan to another.

The accuracy of the theoretical values of reflectance of aluminum and transmittance of sapphire was checked by actual measurements made on the aircraft and in the laboratory. On the aircraft during one of the flights a few measurements were made using the filter radiometer with and without the plate of sapphire in front of it. Measurements on the sapphire plate were also made in the laboratory with a Beckman DK2A spectrophotometer and the Perkin-Elmer monochromator. The reflectance of the specular mirror for various angles of incidence was measured in the range .3 to 2.5μ using a DK2A with the Gier Dunkle attachment.

Computed values of the attenuation due to the atmosphere are available in literature[18] as stated in Part I of this report (Table 3). These values are valid for the U. S. standard atmosphere. Thirteen of the Leeds and Northrup charts of the flight of August 10 in the photomultiplier range were analyzed using the manual data reduction method to check the validity of the theoretically computed atmospheric attenuation coefficients. The deflections of the pen were read for 77 selected wavelengths. The values were plotted manually in terms of $\log_{10}$ of deflection versus air mass, and the points were joined by the best fitting straight line for each wavelength. The atmospheric attenuation and the signal for zero air mass were determined from the slope and zero intercept respectively of these graphs. These Langley plots for 8 of the wavelengths are shown in Figure 25. Figure 26 gives the values of atmospheric attenuation at the selected wavelengths. The Y-axis in Figure 26 is the percentage ratio of the spectral energy transmitted normally to the altitude of the aircraft to that incident above the atmosphere. The results of these computations of atmospheric attenuation were used to correct the theoretical values of Table 3, and to prepare a revised table which was used in the computerized data analysis of all the solar scans made by the Perkin-Elmer and Leiss monochromators.

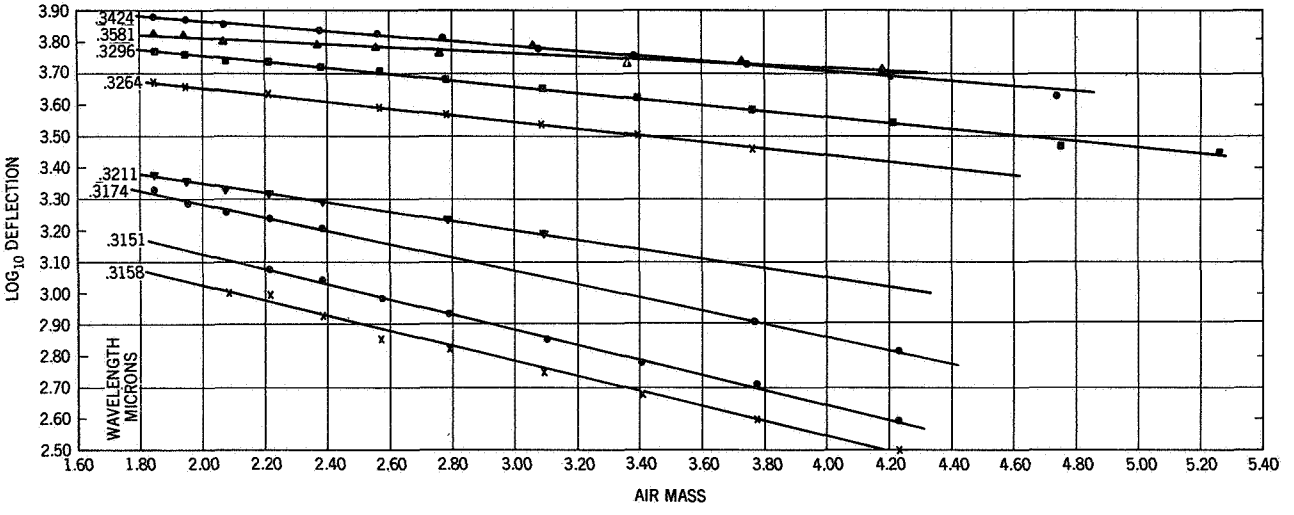

Figure 25—Log_{10} deflection of Perkin-Elmer vs. air mass.

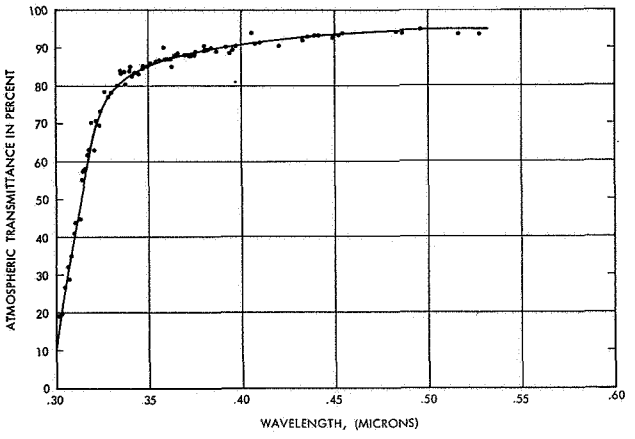

Figure 26—Atmospheric transmittance versus wavelength from Perkin-Elmer.

The manual data reduction method was used also to obtain the solar spectral irradiance at the 77 selected wavelengths, based on the Perkin-Elmer scans of August 10. The detector signals for zero air mass obtained from the Langley plots were corrected for reflection of the specular mirror and transmittance of the aircraft window. The spectral irradiance was computed at these wavelengths using Equation (6) with the necessary correction for solar distance. The curved lines showing irradiance in absolute units in Figure 23 are based on these computations.

The manual data reduction method is obviously too time consuming, and further does not take into account the finer details of the Fraunhofer structure of the solar spectrum. Hence a computer program was prepared for handing the data recorded on the magnetic tapes and calculating from each spectral scan the solar spectral irradiance for zero air mass. The following operations are performed. The analog signals of drum voltage, gain setting and detector signals are read every 1/5 second of scanning time, values are converted from analog to digital, and five successive values are averaged. From initial and final values of drum voltage, the individual scans are recognized. The signals are converted to a uniform gain setting of 20. Drum voltage is converted to the drum reading and thence to wavelength. The correction factors for the atmosphere, window, and mirror are computed at each wavelength, as also the irradiance and signal of the standard lamp by interpolation from tables supplied to the computer. Spectral irradiance at each wavelength is calculated from Equation (6). The integrated values of the irradiance over bands of designated width are computed. For most of the scans the bandwidth chosen was 100 A for the photomultiplier range and 1000 A for the thermocouple range. For a few selected scans and over limited wavelength ranges the integrated area under the spectral curve was computed also for bandwidths of 10, 5, 2 and 1 Ångström, thus to display more clearly the Fraunhofer structure. The program provides for a printout of the energy in each band, the integrated value of the energy up to the end of that band, and for normalization with reference to a standard solar irradiance curve. The standard chosen was the Johnson curve.

A total of 71 spectral scans of the sun were thus reduced. The data from some 30 percent of the scans could not be used for the final average for various reasons such as frosting of the aircraft window, cirrus clouds above the aircraft, maladjustment of the mirror system, roll of the aircraft or changing of magnetic tapes during a scan. The data from the other scans were in fairly close agreement.

The final results are presented in Figures 27, 28 and 29. The computer generated graphs and tables were the main source for the preparation of these figures. Some of the fine structure was added by comparison with the Leeds and Northrup charts. Figure 27 covers the range .3 to .42 μ

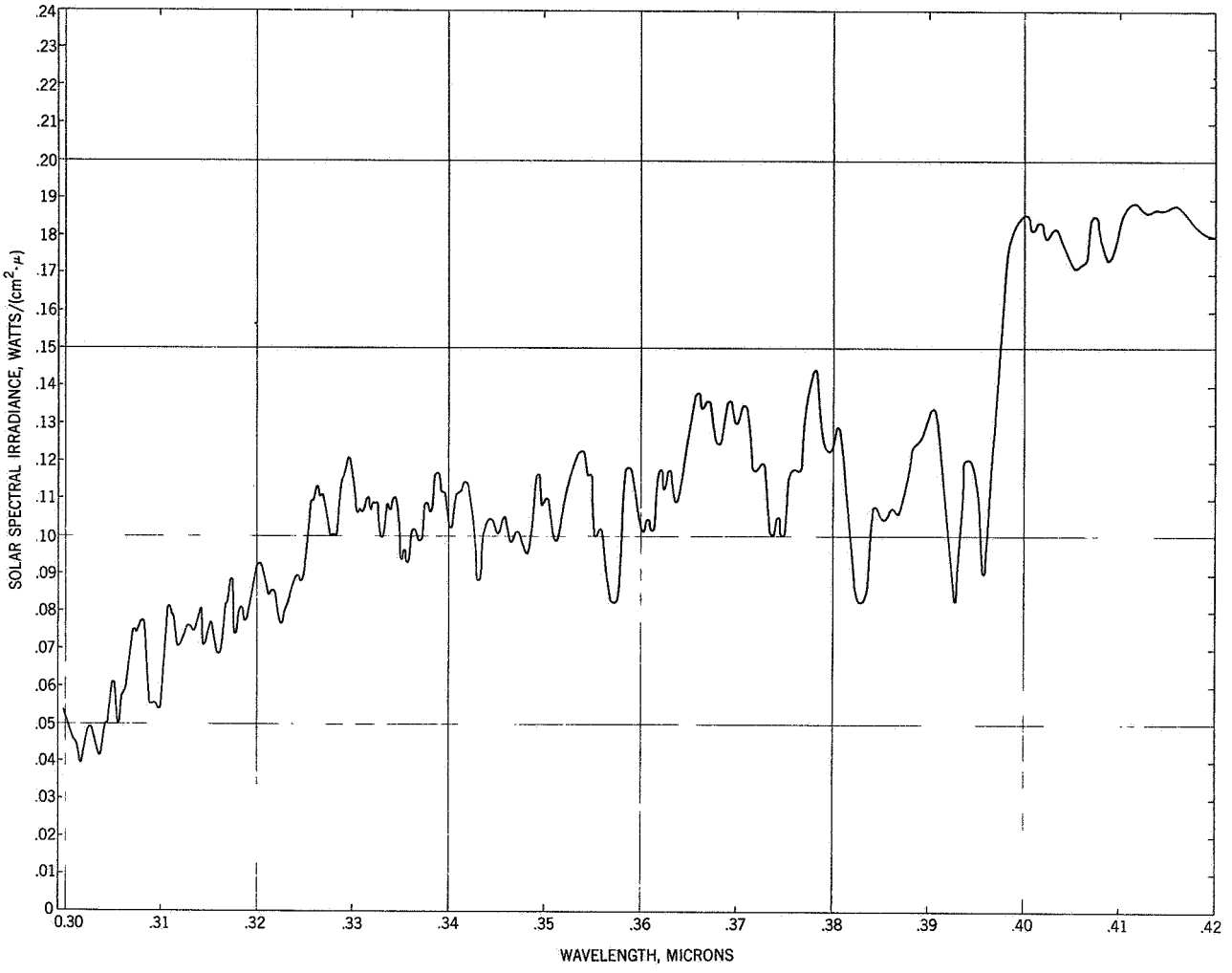

Figure 27—Perkin-Elmer data in the range .3 to .42 μ.

where the Perkin-Elmer has maximum wavelength resolution, and Figure 28 covers the rest of the photomultiplier range. These figures present essentially the same data as the Leeds and Northrup chart shown in Figure 24, with this difference that the wavelength increases from left to right and that the wavelength scale and irradiance scale are linear. The data from the thermocouple range are shown in Figure 29 by the circles with centered dots. The black dots refer to the results from the P-4 interferometer discussed in Part III, section E, and the crosses refer to F. S. Johnson's curve.[1] The results in the range of wavelength longer than 2.3 μ are included in the final Table 5 and in the figures which represent a weighted average of all the spectral irradiance instruments.

The wavelength resolution of the Perkin-Elmer system was determined by two independent methods, first by measuring the half widths of very narrow emission lines of mercury with different slit widths and secondly by comparing the half widths of the H and K lines of calcium as seen on our Leeds and Northrup charts and in the Utrecht Altas.[29] The two values were in close agreement. The half-width of the lines increases from relatively small values of 2.7 A at 3000 A and

4.4 A at 3500 A to 11 A at 5000 A. The wavelength resolution, $\lambda/\Delta\lambda$, where $\Delta\lambda$ is the observed half-width or instrumental profile, decreases from 1100 at 3000 A to 455 at 5000 A. In the thermocouple range where the slit-width is 20 times greater, the resolution is considerably less; it increases from 11 at 7000 A to 90 at 4 μ.

The major sources of error are scattered light from the roof of the aircraft shining on the diffuse mirror and the small degree of instability in the positioning of the mirror directly in front of the thermocouple detector. Detailed analysis of the solar and calibration scans made at different times and both in the laboratory and in the aircraft was made to determine the magnitude of this error. It is estimated that the accuracy of the spectroradiometric measurements is about ±5%.

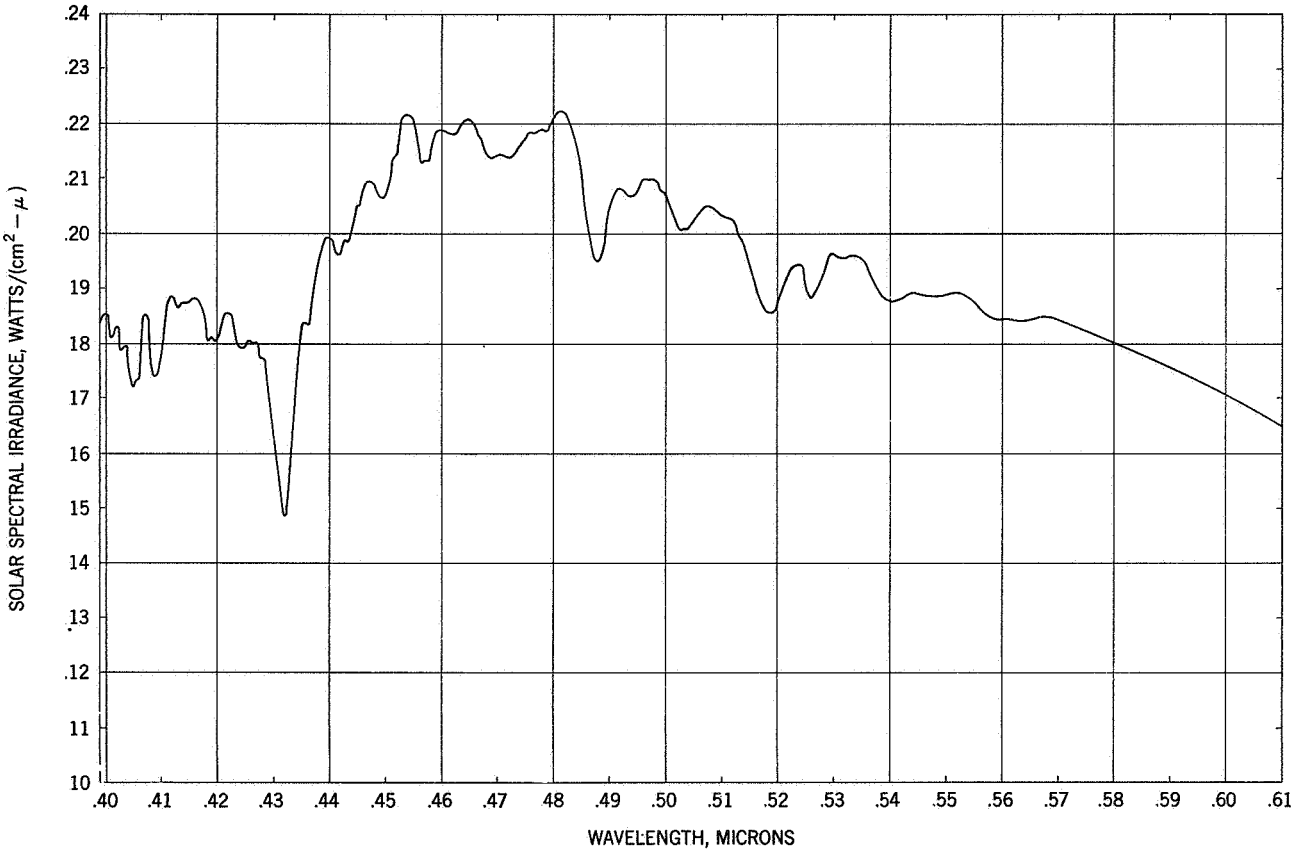

Figure 28—Perkin-Elmer data in the range .4 to .61 μ.

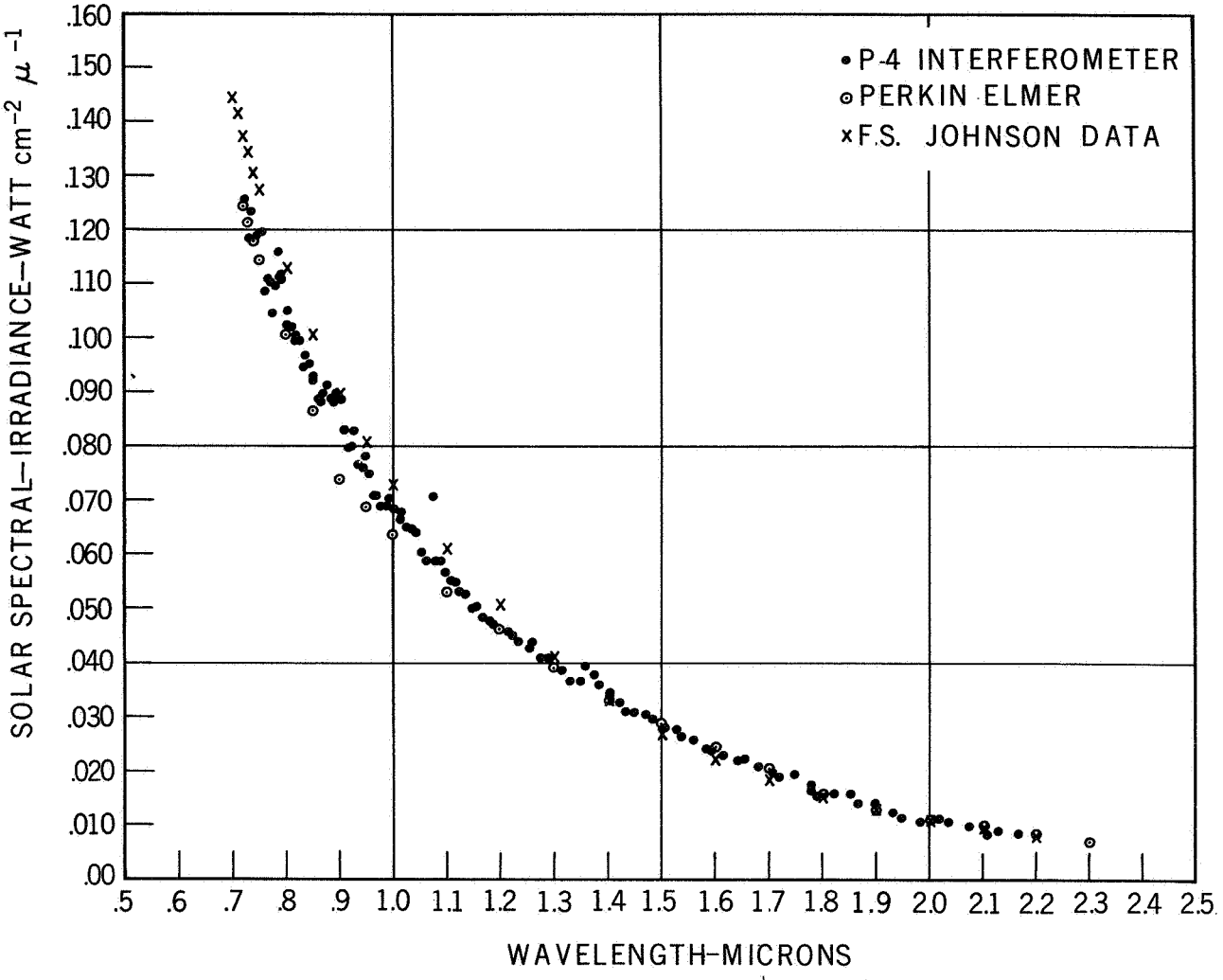

Figure 29—Solar spectral irradiance in the infrared range 0.7 to 2.5μ, Perkin-Elmer and P-4 data.

B. LEISS MONOCHROMATOR

R. McIntosh and S. Park

1. DESCRIPTION OF THE EQUIPMENT

The three following sections discuss the spectral irradiance instruments which were operated by the Thermophysics Branch, Spacecraft Technology Division, GSFC. They are a Carl Leiss double prism monochromator, an Eppley Filter Radiometer and an ITT Electronic Scanning Spectrometer. Each instrument was designed for observing the solar beam through the upper aircraft windows for solar altitudes ranging from about 20° to 70°. No auxiliary mirrors were employed as each instrument was mounted on a pseudo-polar axis in such a manner that an integrating sphere intercepted a direct beam of solar radiation which after diffusion completely filled the optical aperture of each spectral instrument.

A description of each instrumentation system is given, along with the results and some comparisons to previous ground-based measurements.

The Carl Leiss double prism monochromator was used for a total of forty solar scans, each from .3 to 1.6 microns. The relative spectral distributions were in good agreement with published values and with the filter radiometer discussed in section C. However, calibration difficulties necessitated a normalization to the energy value obtained from the total irradiance measurements, 135 mw cm^{-2}.

The Leiss monochromator is a double prism instrument designed to provide high dispersion and minimal stray light. The instrument used in this experiment (see Figure 30) was equipped with two ultrasil quartz prisms. The three slits (entrance, intermediate, and exit) were set wide enough to provide sufficient energy while maintaining good resolution.

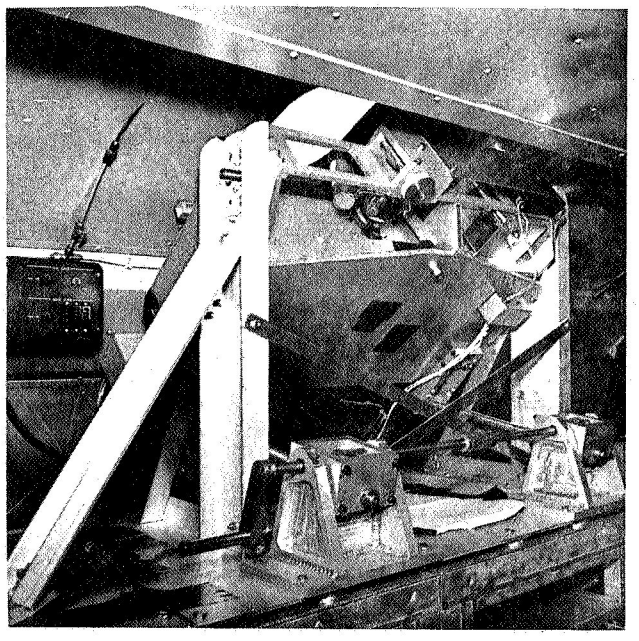

Figure 30—Mounting of the Leiss monochromator.

The Leiss was designed as a laboratory instrument. Therefore, some modification was necessary to make it suitable for an airborne experiment. The mirror and prism mounts were stiffened and the entire instrument was enclosed in a rugged, light-tight aluminum box having sufficient strength to provide for mounting in a cradle which could be swung by a gearing mechanism on its longitudinal axis to allow solar tracking. The housing also provided a heat sink and air current insulation. Provision was made for thermostatic temperature control through the use of heating coils mounted inside the housing.

Two detectors were used—an EMI 9558 QA photomultiplier tube for the UV and visible regions and a Kodak Ektron lead sulfide cell for the IR. These detectors were mounted in an auxiliary light-tight box secured to the primary instrument housing. The detectors were mounted so that they could be quickly interchanged by rotating a lever. For maximum stability the PbS cell was thermoelectrically cooled to a constant temperature of approximately 0°C. The EMI tube was chosen for its low noise and dark current, extended red response, and high sensitivity.

A three inch diameter integrating sphere was coated with a GSFC developed magnesium oxide (MgO) paint and then lightly smoked (1-2 mm) with magnesium oxide. The paint was used instead of a thick smoked coating because it was felt that the shock and vibration within the aircraft might damage a smoked coating because of its very fragile nature. The sphere was positioned so as to provide a diffuse source of illumination for the entrance slit of the monochromator. It was mounted

on an axis perpendicular to the plane of the entrance slit and could be rotated by means of a hand driven worm gear to observe either the sun or the standard of spectral irradiance. This adjustment was at right angles to that of the main elevating mechanism and provided the second degree of freedom for tracking the sun. The use of the sphere also minimized the effects of roll and yaw of the aircraft.

The sphere was positioned immediately behind the aircraft window where it intercepted the direct solar beam, thus eliminating the need for any mirrors. The determination of the reflectance characteristics of such mirrors as a function of angle of incidence is often difficult and tedious, and the additional frame design requirements necessary to directly view the sun were felt justified.

The alignment of the monochromator on the sun was accomplished by using a six inch long tube with a pin hole and graduated target. This tube was attached directly to the sphere. The operator manually adjusted the elevation and azimuth angles of the monochromator. Figure 30 shows in detail the sphere and cranking mechanism, as well as the mounting frame used to support the equipment. The working standard lamp and housing can also be seen.

The wavelength drum which rotates the prisms was operated by a small ac synchronous motor and gear drive at one rpm. This made it possible to make one complete measurement (.3 to 1.6 microns) in five minutes (including the changing of detectors). Wavelength markers were produced on the strip chart recordings by means of a cam and relay attached to the drum.

2. ELECTRONICS

The electronic instrumentation for the Leiss consisted of the following components: a Brower model 129 synchronous amplifier tuned to 33 Hz, a specially built chopper and electronics module mounted inside the Leiss following the intermediate slit, a Power Designs model 5165 high voltage power supply, a Leeds Northrup Type G Speedomax recorder, an E. G. and G. Thermoelectric module power supply, and various control and monitoring circuits. The high voltage power supply used to drive the photomultiplier tube has a voltage stability of .001% resulting in a tube constancy of better than 1%.

The electronics for the Leiss as well as for the filter radiometer and the ESS were wired into an Elgar model 3001 transient regulator.

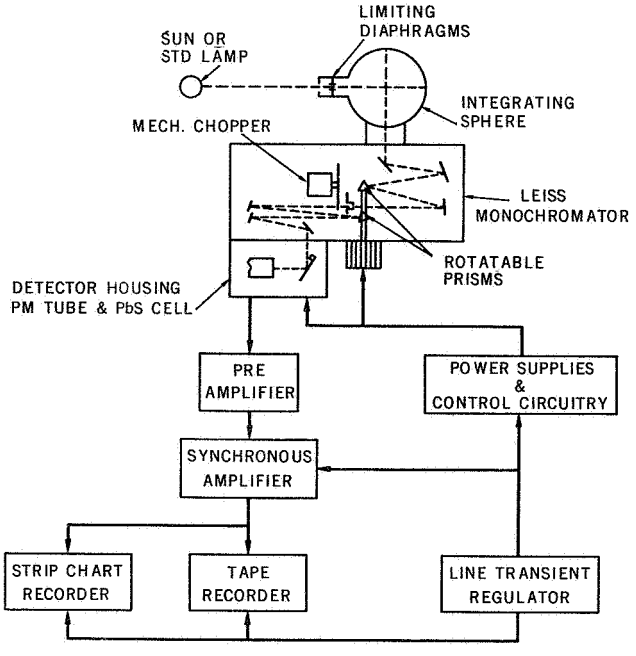

Figure 31—Block diagram of the instrumental setup of the Leiss monochromator.

This was done because the aircraft's power converters were somewhat noisy and not regulated well enough for some of the instruments. The standard lamp power supply was wired into a Sorenson line voltage regulator which provided extremely stable lamp operation.

Figure 31 shows a block diagram of the entire instrumentation arrangement.

3. CALIBRATION

The calibration of the Leiss was accomplished through the use of a 1000 watt NBS type of standard of spectral irradiance.[30] A certified standard (Eppley no. 1145) was employed for the basic calibration. Another lamp of the same type was used as a working standard and mounted in an aluminum box on the Leiss frame. The lamp current was monitored with a calibrated shunt and digital voltmeter and could be easily maintained to within .01 amp. Since the working standard was mounted inside an aluminum box its irradiance was somewhat higher than that of the primary standard because of the reflectance of aluminum and the slightly higher operating temperature of the lamp. This was very helpful in the ultraviolet where the irradiance of these lamps falls off rapidly. Monochromator calibrations were performed in flight as well as on the ground.

4. DATA ANALYSIS

Data were taken for each of the flights—a total of 40 measurements. However, only data from flights two through five have been analyzed. After the first flight the slit settings were changed significantly to improve resolution. Therefore, these data are not included here. The data from the final flight were not used because of an error in flight calibration. Several other runs were discarded because of cloud cover and instrument difficulties. The results from the remaining nineteen measurements are presented here.

During the flights the calibration signal appeared to drift, especially in the ultraviolet region. All efforts to correct this difficulty in the field were futile. After the expedition, a large number of measurements were made to determine the exact cause of this drift, but thus far it has not been discovered. Since the repeatability of the working standard was verified, the drift was almost certainly caused by some heating effect in the Leiss optical system. It is interesting that the drift was quite reproducible (within 1%) as a function of time. Fortunately, no such drift could be observed in the solar data, or in any of the data from the filter radiometer or ESS which used similar instrumentation.

Because of these difficulties it was impossible to obtain absolute measurements of the solar spectral irradiance from these data. Therefore all of the data obtained by the Leiss were normalized to the value of the total irradiance of the sun as measured by the total irradiance instruments —135 mw cm^{-2}. Since the value represents the total energy of the sun and the Leiss covered only the wavelength range .3 to 1.6 microns, it was necessary to normalize the data to the energy in that range only. For this purpose the values of Gast[15] were used for the energies above and below.

These are 2.44 and 14.2 mw cm^{-2}. The energy in the range .3 to 1.6 microns is therefore 118.4 mw cm^{-2}. The technique used for reducing the data was essentially the same as for the Perkin-Elmer monochromator. Thus, the spectral irradiance of the sun for zero air mass was computed at each of the flexion points of the Leeds and Northrup chart, the area under the curve of spectral irradiance versus wavelength was integrated over the wavelength range .3 to 1.6 microns and the normalization was performed using the value 118.4 mw cm^{-2}.

5. RESULTS

The Leiss results are depicted in Figures 32, 33 and 34. Figure 32 is a comparison of the Leiss, filter radiometer, and Perkin-Elmer. As can be seen, the agreement is good between the Leiss and the filter radiometer. Figure 33 compares the Leiss data to the most recent ground

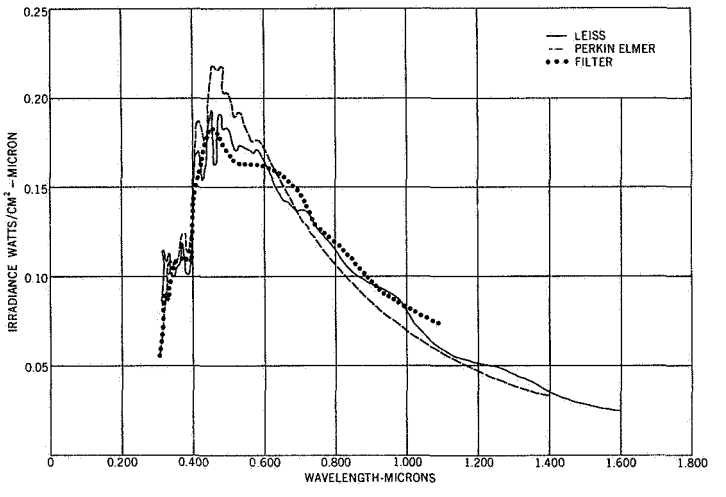

Figure 32—Comparison of Leiss, Perkin-Elmer and filter data.

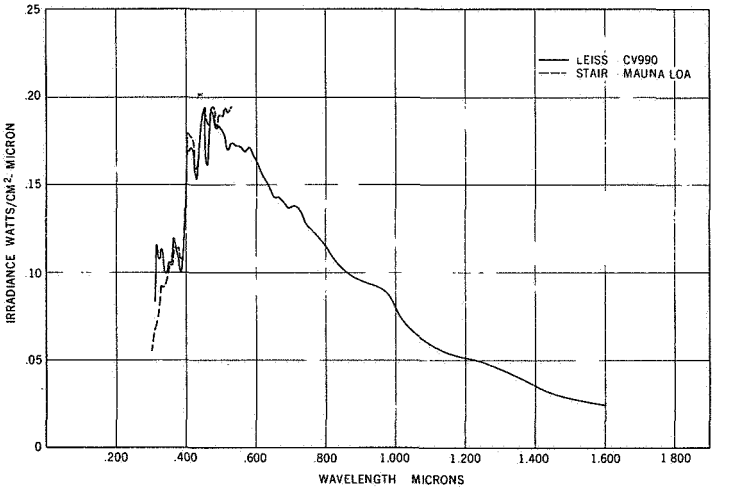

Figure 33—Comparison of Leiss and Stair (Mauna Loa) data.

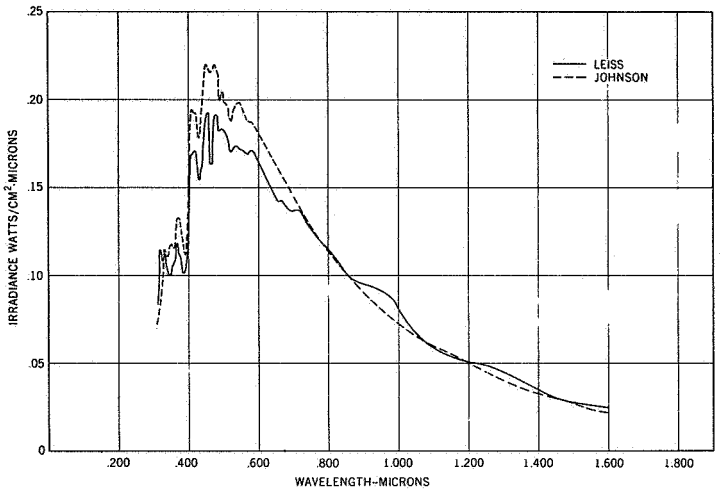

Figure 34—Comparison of Leiss and Johnson data.

based measurements of Stair[31] at Mauna Loa, Hawaii. The agreement here is again good in the ultraviolet region. Figure 34 compares the Leiss data to that of Johnson.[1] The fact that Johnson's visible spectrum is higher is due partly to his higher total irradiance value of 140 mw cm^{-2}. The 5 mw difference occurs primarily in the visible region.

Two interesting features appear on the Leiss data. These are the two humps in the curve at about .9 and 1.3 microns. None of the previously reported data shows this. However, very little data is available for this region of the solar spectrum. Attempts have been made to account for these anomalies on the basis of a possible system error, but after careful examination this does not seem to be the case.

An estimate of the errors involved in the measurements is as follows:

Error in total irradiance (from Ångström Pyr.)	±3%
Error in irradiance outside wavelength interval .3-1.6μ	±4%
Error due to window transmittance	±1%
Instrumentation error	±2%

The total RMS error is 5.5%.

C. FILTER RADIOMETER

R. Stair, J. J. Webb and D. L. Lester

INTRODUCTION

A GSFC modified Eppley Mark V filter radiometer was used to make solar spectral measurements from .3 to 1.1 microns. Good agreement has been noted with the Leiss and with recent ground based measurements.

1. DESCRIPTION OF EQUIPMENT

The basic mechanism for an Eppley Mark V radiometer was employed in the design of a photoelèctric filter wheel radiometer. No commercial instrument of the required type was available. The thermoelectric detector, shutter and shutter drive, and other features not associated with the filter rotation mechanism were removed, or made non-active. The filter wheel rotation mechanism provided for the step rotation of two filter wheels, each containing 13 filter positions. Allowing for a zero position and for the interposition of two wide band filters or radiation (or isolation) screens, a total of 22 narrow band filters could be installed on the two wheels at one time. Such filters were set up on two wheels for use with an RCA type 935 phototube (S-5 response) to cover the ultraviolet (11 filters) and visible (11 filters) within the range of 3100 to 6000 A. On a third wheel another set of 11 filters was arranged to cover the spectral range from 6000 to 11,000 A. This latter set, together with those for the visible range, was used with an RCA type 917 phototube (S-1 response). Thus, to shift the instrument coverage from the ultraviolet and visible to the visible and near infrared required the changing of one filter wheel and the interchange of detectors. Since this procedure required a significant amount of time, it was decided to use only one combination during any particular flight. This procedure was followed except that during the flight of August 16, the constant air mass flight, both ranges were covered by making the change at mid-flight.

The narrow band interference filters supplied by Eppley were chosen to cover the spectral range mentioned above. In the ultraviolet, each filter has a half-band width of approximately 100 A and is centered at an even wavelength, e.g., 3100, 3200, 3300, etc. to 3900 A. Those at longer wavelengths have wider half-band widths and in general, are also centered on even wavelengths spaced at 500 or 1000 A in the visible and infrared. Thus, each filter (except for several wide band filters) covers a portion of the solar spectrum extending in either direction from its central transmission peak such that, ideally, where the transmittance of one filter drops to one-half its value, the next has increased to one-half its value. The transmittance of each filter was measured on a Beckman DK-2A spectrophotometer.

2. INSTRUMENT MODIFICATIONS

The Eppley mechanism was originally designed for manual operation in changing filters. This consisted of momentarily pressing a push button switch for a single filter position change or by retaining the switch in the closed position until the desired filter was in place. Automatic operation could be had through fixing this switch in the closed position. This, however, leaves each filter in position for only a very short time (about one second or less) which is insufficient for precise recording. To alleviate this situation, a timing motor was set up to momentarily close a microswitch, wired across the button switch, once each 8-1/3 seconds, thus providing for automatic filter changes at that time interval.

The instrument was mounted in the aircraft in a frame similar to that used for the Leiss, i.e., a pseudo-polar axis mount. The mounting arrangement is shown in Figure 19. As with the Leiss,

a manual elevating mechanism provided instrument adjustment for solar altitude and a worm gear mechanism rotated the integrating sphere. The sphere was the same size and used the same coating as the Leiss. A block diagram of the instrumental arrangement is shown in Figure 35.

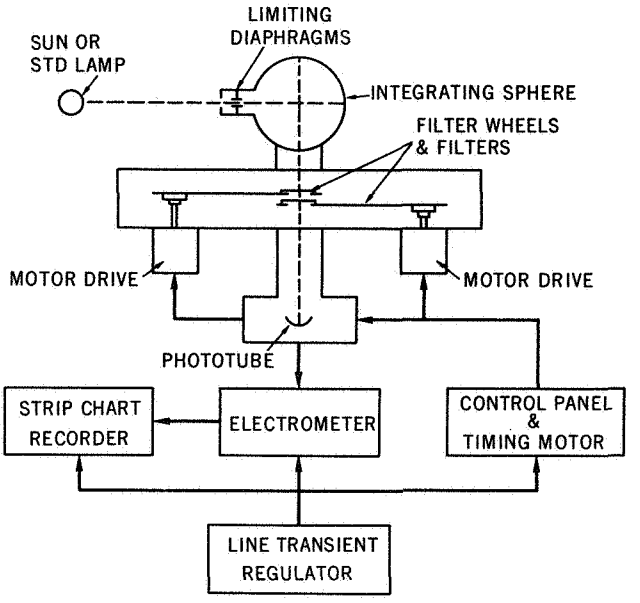

Figure 35—Block diagram of the instrumental set-up of the filter radiometer.

3. ELECTRONICS

The primary electronics used with the filter radiometer consisted of a Keithley model 610 R Electrometer and a Moseley model 7100B strip chart recorder. The current from the phototube was amplified by the electrometer and directly recorded by the Moseley. No modification of either instrument was required as each has several sensitivity settings.

4. CALIBRATION

Calibration was accomplished in the same way as with the Leiss. A 1000 watt NBS type quartz iodine standard of spectral irradiance was mounted in an aluminum box and attached to the instrument frame. The housing can be seen in Figure 19. The only difference in procedure was that with the filter radiometer wavelength calibration was not a problem since the filters themselves provided the wavelength range.

5. RESULTS

The analysis involved in reducing the filter radiometer data is detailed and somewhat complex and will not be described here. The procedures and techniques used can be found in a recent Goddard contract report.[32] The results presented here are also taken from this report.

The zero air mass solar spectral curve is shown in Figure 32, along with the results of the Leiss and Perkin-Elmer measurements. The comparison with the Leiss is very good in all but the regions around 3000 and 6500 A. It is believed that these discrepancies are due to calibration uncertainties. The fact that the results of the two instruments agree closely despite their differences in optical characteristics seems to strengthen their validity. Also, the energy scale for the filter radiometer was obtained from the in-flight calibrations, not from normalization. Thus it seems that the normalization procedure was justified for the Leiss.

Figure 36 shows a comparison of the filter radiometer and the most recent ground based measurements available, those of Stair at Mauna Loa. A good agreement is again noted.

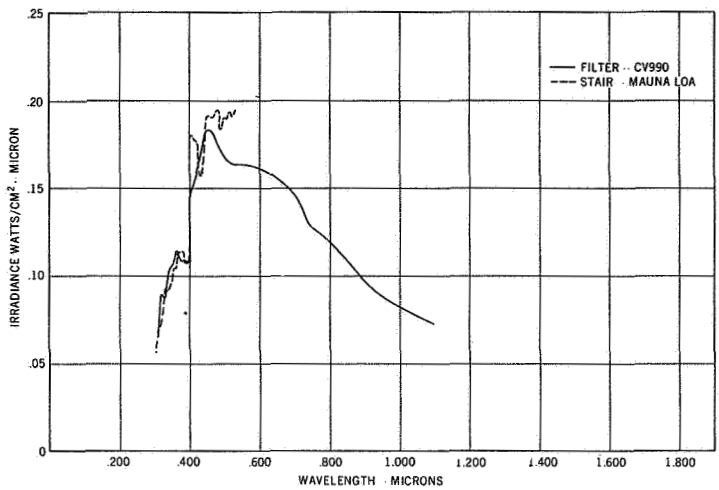

Figure 36—Comparison of filter radiometer and Stair (Mauna Loa) data.

An uncertainty of approximately 5% is estimated, due mainly to the inaccuracies of the standard lamp and window and filter transmittance values.

D. ELECTRONIC SCANNING SPECTROMETER

J. J. Webb

INTRODUCTION

An Electronic Scanning Spectrometer recorded solar data from 3000 to 4800 Ångströms during all six NASA 711 flights. A total of 95 spectral runs were obtained, but only 17, randomly selected, were used in the data analysis. Resolution was not as good as expected, and the spectral energies are lower than results of other experimenters.

1. DESCRIPTION

The Electronic Scanning Spectrometer (ESS), manufactured by ITT Industrial Laboratories of Fort Wayne, Indiana, is designed to measure either static or rapidly changing spectral distributions in the ultraviolet and visible regions from 2500 Å to 5000 Å. Completely electronic and weighing only 21 lbs., the spectrometer scans the spectrum by means of a television-type camera tube called an image dissector. A long narrow slit aperture in the tube serves as the exit slit of the optical unit, which consists of two turning flats, a focussing mirror, and a grating, (see Figure 37). A photoemissive surface (S-21) on the faceplate converts the optical spectrum into an electron spectrum within the vacuum of the tube. The electron image is formed within the tube in the plane

of the tube's slit aperture. The sampling of the spectrum takes place by sweeping the electron image across the slit aperture by means of magnetic fields generated by coils surrounding the tube. The signal is then amplified in the tube exactly as in conventional photomultipliers.

2. INSTRUMENT MODIFICATIONS

In order to adapt the instrument for solar measurements aboard the aircraft certain modifications had to be made.

The rapid scanning feature was changed to a much slower speed because of a lack of a suitable recording device. The scanning was done by driving the field coils with a potentiometer and synchronous motor which took about two minutes for one complete scan of the wavelength region.

An integrating sphere like those used with the Leiss and Filter Radiometer was mounted in front of the entrance slit.

A mechanical chopper was also installed in front of the entrance slit to allow the use of a tuned amplifier.

As was the case with the Leiss and filter radiometer, the ESS was mounted on a pseudo-polar axis and two degrees of freedom were provided for manual solar tracking.

A photograph of the actual flight configuration is shown in Figure 38.

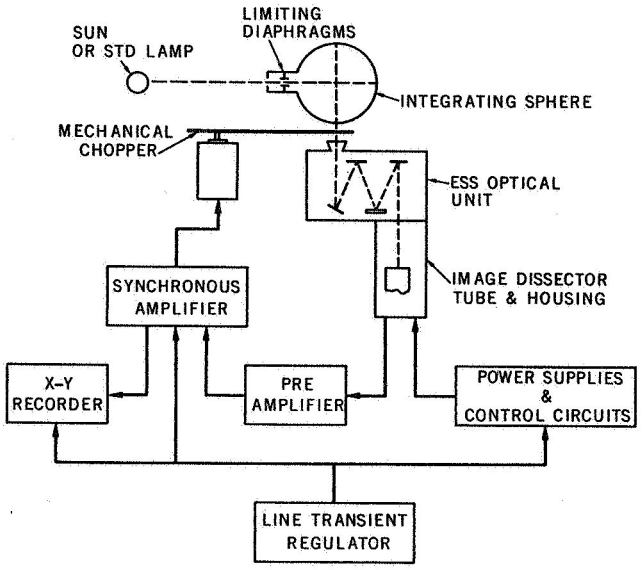

Figure 37—Block diagram of the instrumental set-up of the ESS.

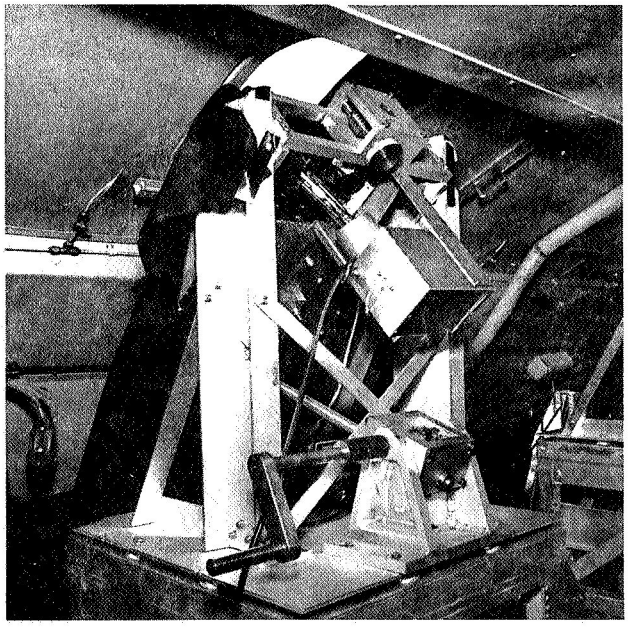

Figure 38—Mounting of the ESS spectrometer.

3. CALIBRATION

Wavelength calibration and indexing was performed by using a low pressure Spectroline Cadmium lamp whose spectrum is well know and adjusting the time of the scan to align the spectral lines with the appropriate linear markings on the chart paper. For solar measurements the Fraunhofer lines provided excellent wavelength identification. Intensity calibrations were accomplished in the same way as those for the Leiss and Filter Radiometer, i.e., with a 1000 watt quartz iodine lamp.

The calibrations were made in flight prior to the solar data recording, and also on the ground between flights. These data agreed fairly well and an average calibration curve was determined and used in the solar data analysis.

4. RESULTS

The data were not as good as expected primarily for two reasons, poor resolution and unreliable wavelength calibrations.

The addition of the integrating sphere was done just prior to the flights and no time was available for a thorough ground test. Apparently the sphere reduced the resolution from a previous 10 Ångströms[33] to 35 Ångströms by filling the optics in a different manner. Had the ESS been equipped with a variable entrance slit, the resolution could easily have been improved. However, the instrument was made with a fixed entrance slit of either 50 or 100 microns, both of which were too large. Therefore, there was nothing that could be done except observe the poor resolution.

As stated earlier, a total of 95 spectral scans were recorded during the six flights, but only 17 were used in the Langley method[7] of data analysis. Clouds during portions of the flights eliminated some runs, and a lack of time and manpower made it impossible to utilize all of the remaining runs. A random selection of the 17 runs was made, covering the air mass range as well as possible. Voltage readings were chosen from each run at the maximum, minimum, and inflection points. The logarithms of these voltages were then plotted versus the appropriate air masses for each of the chosen wavelenglths. Some typical Langley plots are shown in Figure 39. The data appear to be good, i.e., they lie on straight lines except in the UV region where

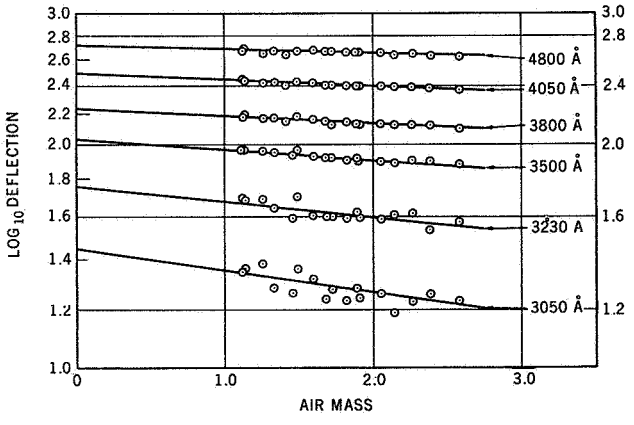

Figure 39—Typical Langley plots from ESS data.

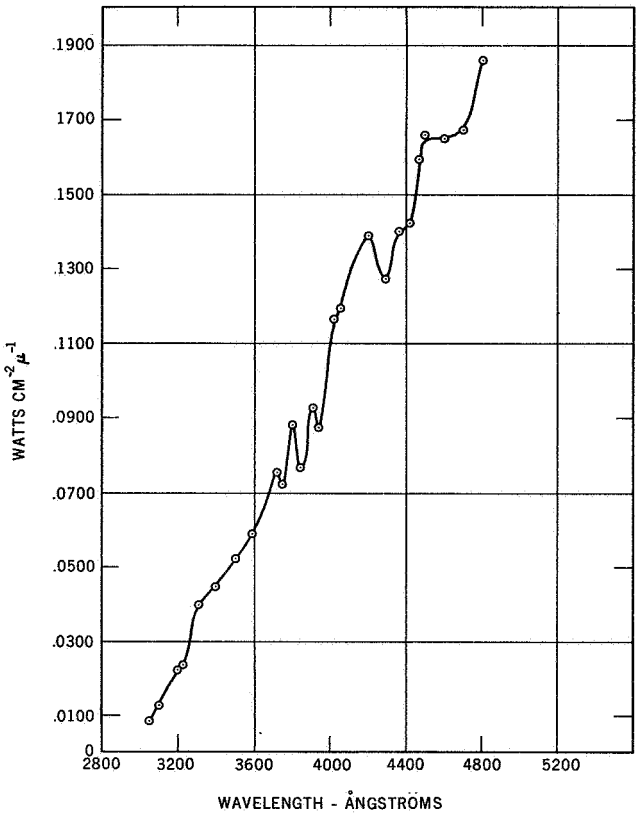

Figure 40—ESS zero air mass solar curve.

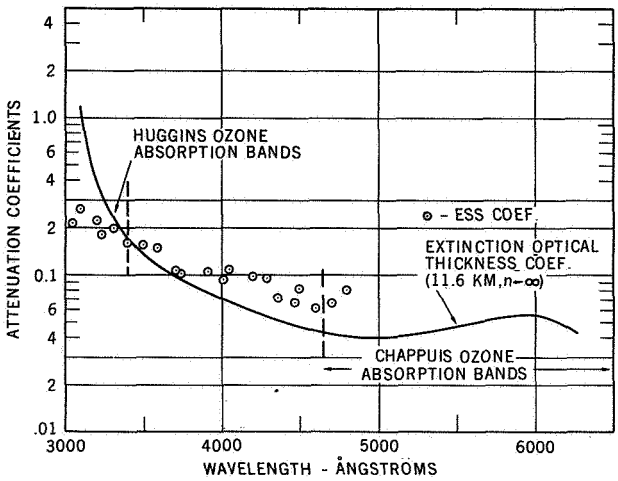

Figure 41—Comparison of experimental (ESS) and theoretical attenuation coefficients.

ozone absorption and low detector sensitivity increased the scatter. A least squares analysis was made for each wavelength and the y intercept (at air mass 0) was determined. These values were then corrected for mean distance to the sun and window transmission, and reduced to absolute values with the calibration data.

A plot of the zero air mass data is shown in Figure 40. Compared to the Johnson curve, the E.S.S. curve is considerably lower in the range 3000 to 4000 Å. It is also somewhat lower than the curves obtained by the Leiss and the filter radiometer.

The data in all other respects appear to be reasonable, including the comparison shown in Figure 41 of the experimental attenuation coefficients (the slopes of the Langley plots) and the theoretical curve of the extinction optical coefficients for a turbid atmosphere[18] at 11.6 Km. The theoretical curve represents Rayleigh and aerosol scattering and ozone absorption. The fact that they do not overlay exactly indicates that the atmosphere above the observers was not homogeneous (an assumption made in the tables).

The in-flight wavelength calibration data did not show good repeatability from day to day, so an average value was used. However, the possibility of a wavelength shift in the data exists and may be a cause of difficulty. In addition, a possible non-linearity in the ramp voltage drive mechanism may be a contributing factor.

Because of these problems, the ESS data were not given any weight in the determination of the final spectral curve presented in the conclusion of this report.

E. P-4 AND I-4 INTERFEROMETERS

J. F. Rogers, P. Ward and M. P. Thekaekara

1. DESCRIPTION OF INSTRUMENTATION

Two interferometer spectrometers were used to cover the spectral range from 0.3 to 15 microns. Both interferometers were manufactured by Block Engineering, Inc., Cambridge, Mass. A Michaelson type, I-4, interferometer covered the region from 2.6 to 15 microns and a polarization, P-4, interferometer measured the spectral band from 0.3 to 2.5 microns.

Although interferometers have been a valuable laboratory tool for many years, their application in the fields of spectroscopy and radiometry has been severely limited until recently because of the difficulty in performing the necessary mathematical calculations. With the advent of easy access to digital computers in the past ten years, the technique of Fourier spectroscopy has received a great deal of interest due to distinct advantages in radiation gathering power and improvement in signal to noise ratio.

Since this is a relatively new field we will discuss some of the basic principles of interferometric spectrometers. Although there are many kinds of interferometers the principle common to all is that the incident radiation is made to selectively interfere with itself revealing information about the spectral energy distribution. Unlike dispersive instruments that isolate and measure a series of narrow spectral bands in succession, interferometers accept and analyze all wavelengths in their operating range at one time. Hence there is a great improvement in signal to noise ratio.

For purposes of illustrating the operation of these instruments the Michaelson interferometer is perhaps the simpler and easier to understand.

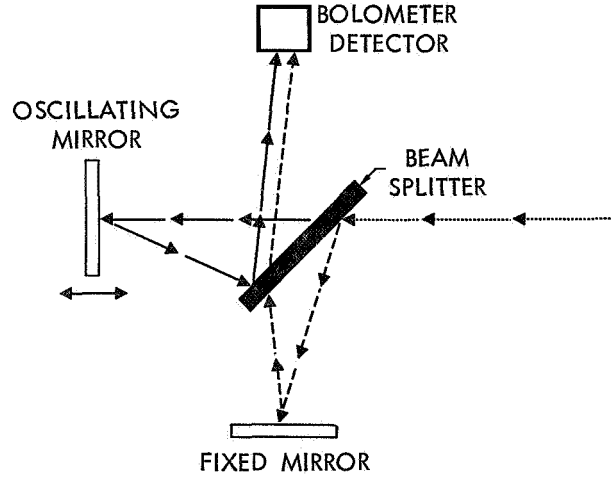

Figure 42—Michaelson interferometer schematic.

Consider a monochromatic ray of wavenumber ν, wavelength λ entering the interferometer, Figure 42. The ray divides into two equal rays at the semi-reflecting beam splitter. Each ray reflects at a mirror and returns to the beam splitter, through which 50% of the energy will be transmitted to the detector. As one of the mirrors moves to and fro with a constant velocity, V, the two rays will interfere with each other constructively or destructively according as the relative path difference is an even or odd multiple of $\lambda/2$. Thus the energy incident on the detector varies periodically. The time interval, τ, between successive maxima of detector signal is time required for the path difference to change by λ, that is, for one of the mirrors to move through $\lambda/2$. Thus $\tau = \lambda/2V$. The modulation frequency of the detector signal is $f_\nu = 1/\tau = 2V/\lambda = 2V\nu$. Thus the output frequency of the interferometer is proportional to the wavenumber of the incident light.

If "white light" radiation falls on the entrance aperture, the output signal will consist of a large central peak at the point of zero retardation when all wave components are in phase plus smaller intensity peaks due to reinforcement of frequency components, ν_i, at mirror displacements that are integral multiples of $\lambda/2$. This output signal is called an interferogram and consists of a linear

superposition of cosine waves that will have the form

$$I(x) = \int_{-\infty}^{\infty} G(\nu) \cos(2\pi\nu x)\, d\nu \tag{7}$$

By the use of Fourier's integral theorem we can transform the above expression to obtain the intensity as a function of frequency. Thus

$$G(\nu) = \int_{-\infty}^{\infty} I(x) \cos(2\pi\nu x)\, dx \tag{8}$$

Equation (8) implies that the interferogram has perfect even symmetry about the zero point and that there is an infinitely large mirror displacement. Since neither statement is true it is necessary to compute both sine and cosine components and to restrict the domain of integration. Let the displacement of the mirror be from $-B/2$ to $+B/2$. The spectrum then has terms

$$P(\nu) = \int_{-B}^{+B} I(x) \cos(2\pi\nu x)\, dx \tag{9}$$

$$Q(\nu) = \int_{-B}^{+B} I(x) \sin(2\pi\nu x)\, dx \tag{10}$$

In terms of these quantities the energy spectrum G is given by

$$G = \left(P^2 + Q^2\right)^{1/2} \tag{11}$$

The phase relationship between frequency components is computed from

$$\phi = \arctan \frac{Q}{P} \tag{12}$$

The phase at the point of zero retardation can be set equal to zero (or 360°) and a change in the direction of net energy flow will then produce a 180° degree phase shift.

The P-4 interferometer operates in a shorter wavelength range .3 to 2.6 μ where the proper alignment of the Michelson mirror system is difficult to maintain. Relative path retardation between the two components is introduced by a Soleil prism. An optical schematic of the instrument is shown in Figure 43. The incident beam is separated by a polarizer into two components of equal

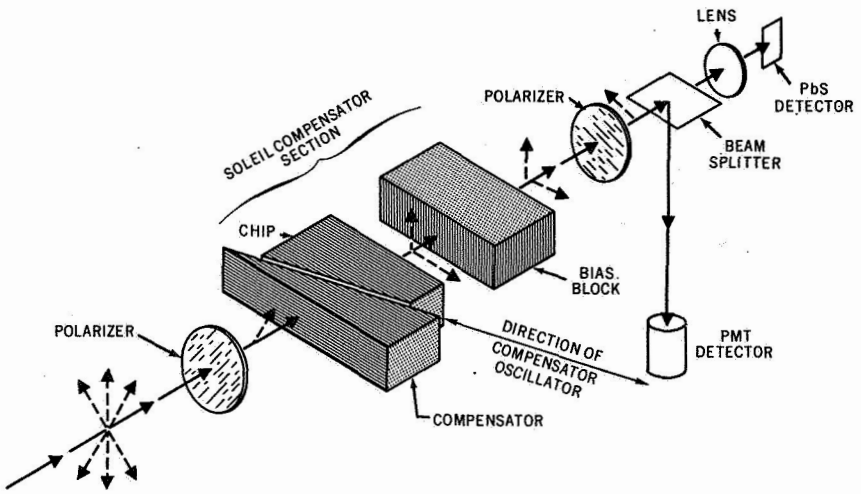

Figure 43—Polarization interferometer schematic.

amplitudes in mutually perpendicular planes. The wave then passes the birefringent Soleil compensator that has a different index of refraction for each wave component; thus the two components traverse the compensator at different speeds introducing an optical path difference between the two perpendicular components given by

$$B = d(n_o - n_e) \tag{13}$$

where d is the thickness of the compensator and n_o, n_e are the indices of refraction in the "O" and "E" planes. The path difference is varied by moving the wedge-shaped section as shown in Figure 43, thus performing the function of the moving mirror in the Michelson interferometer. The radiation is recombined at the second polarizer and then separated at the beam splitter with approximately 90% of the energy transmitted to the lead sulfide detector and 10% sent to the photo-multiplier tube. The resulting interferograms are processed in a manner similar to the method described above.

2. EXPERIMENTAL PROCEDURE

The mounting for the interferometers is shown in Figure 44. It was very similar to that of total irradiance instruments. The

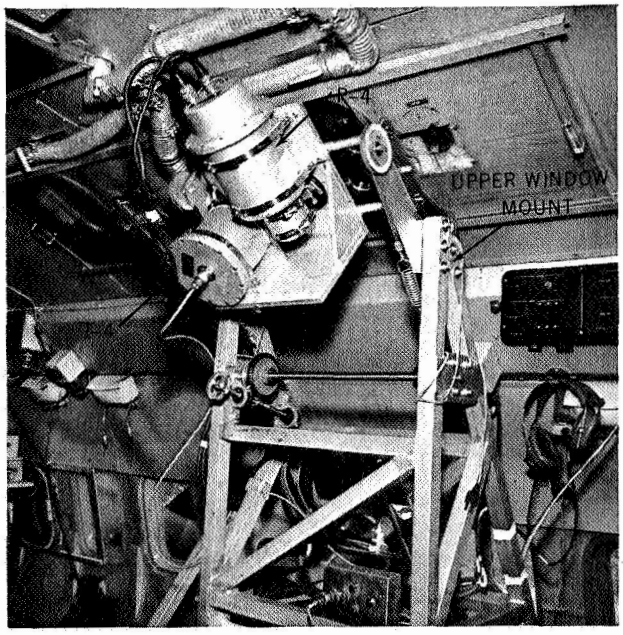

Figure 44—Mounting of the P-4 and I-4 interferometers.

interferometers were aimed at the sun, the I-4 directly, and the P-4 through an integrating sphere and aperture arrangement. The aperture of the P-4 restricted the field-of-view to ±5° in order to minimize sky radiation effects and to be comparable to the other spectrometers and radiometers. The two instruments were mounted side by side with the P-4 viewing the sun through a quartz window and the I-4 through an Irtran 4 window. The output signals were recorded on analog tape while the instruments tracked the sun.

3. I-4 DATA PROCESSING AND ANALYSIS

The analog signals of the interferograms were sampled at constant intervals of path retardation and digitized for computer analysis. One hundred interferograms in succession were co-added to improve the signal to noise ratio for each spectrum. The Fourier transform and phase relationship of each spectral component were then found. A typical amplitude spectrum with the associated phase plot is shown in Figure 45 in terms of output frequency and corresponding wavelength.

At long wavelengths the phase becomes important due to detector radiation. The field of view of the instrument covers an angle of twelve degrees while the sun subtends an angle of only one-half

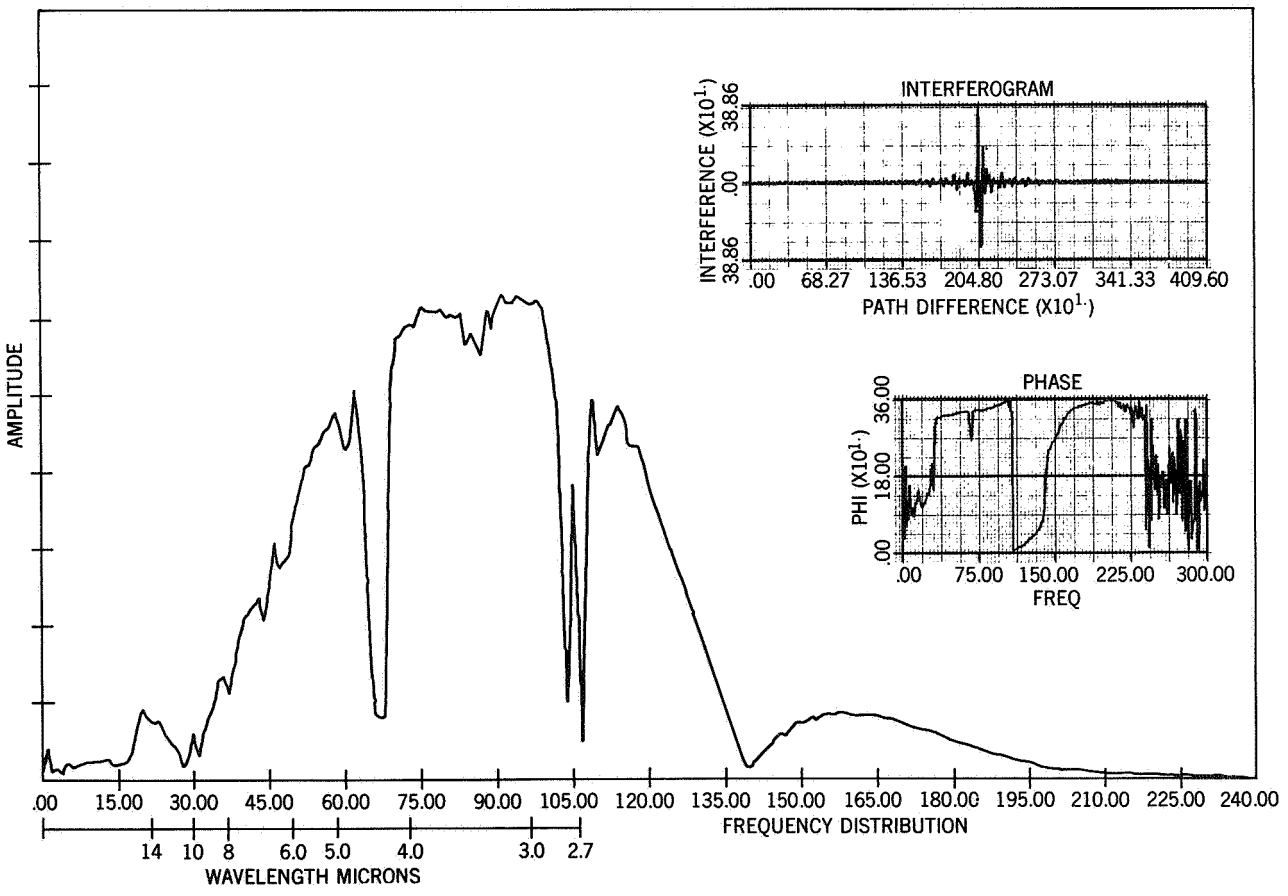

Figure 45—Data from the I-4 interferometer

degree. The thermostatically controlled thermistor bolometer operates at 37°C and therefore radiates energy to the cold sky about the sun and the window frame. This detector radiation becomes an increasingly large fraction of the net energy interchange as we approach the longer wavelengths. At wavelengths longer than 10 microns the net energy is directed out, i.e., the detector radiates more energy than it receives from the sun.

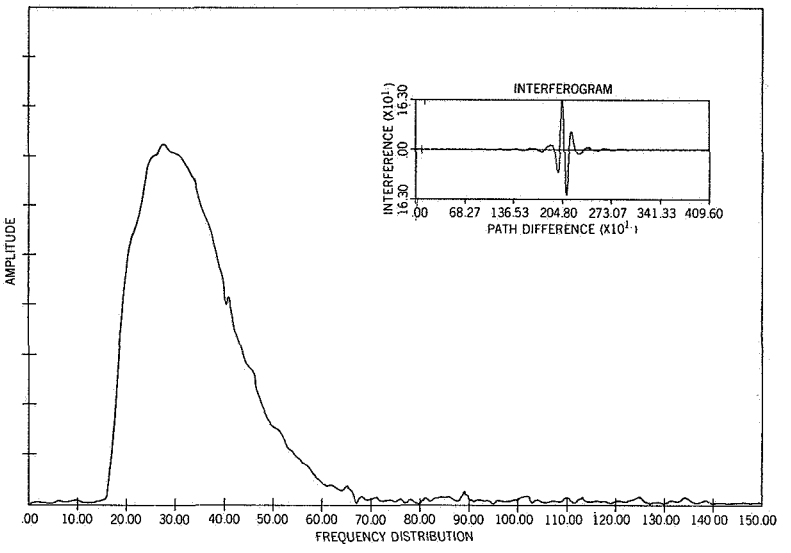

Figure 46—Data from the I-4 interferometer pointed away from the sun.

To account for the detector radiation, a series of measurements were taken while the instrument was pointed away from the sun. Figure 46 is the reduced data from one such measurement. The energy calibration was obtained with a blackbody source manufactured by Infrared Industries, Santa Barbara, Cal. It was run at a temperature of 1200°K with a 1.53 cm. diameter aperture at a distance of 87 cm. from the I-4. The effect of detector radiation was negligible during the calibration runs since the front plate of the source had a temperature of 35°C.

The transmittance of the Irtran 4 window as a function of wavelength and angle of incidence was obtained by viewing the blackbody source with the I-4 through the window. All the data was incorporated into a computer program that solved the equation

$$I_\lambda = \frac{\left[S_{(BKG)_\lambda} \pm S_{(meas)_\lambda}\right] \times I_{(BB)_\lambda}}{T_{\alpha,\lambda} \times S_{(BB)_\lambda}} \qquad (14)$$

where $S_{(BKG)_\lambda}$ is the signal obtained from the background run at wavelength λ; $S_{(meas)_\lambda}$, the signal while viewing the sun; $I_{(BB)}$, the irradiance on the aperture of the I-4 due to the calibration source; $S_{(BB)}$ the signal due to $I_{(BB)}$; and $T_{\alpha,\lambda}$ is the transmittance of the Irtran 4 window as a function of angle of incidence α, and wavelength λ.

The plus or minus sign is used according as the net energy transfer is directed into the instrument or out of it, as is shown by the phase. Ideally the phase should be constant except for the 180° phase reversals but noise in the signal, slight errors in locating the center of the interferogram, and dispersion in one of the optical paths, will produce departures from constancy. Since the data was automatically reduced, a phase-referencing system was adopted whereby the phase at 3.6 microns (in the short wavelength region and removed from major absorption bands) was used as a reference. If the phase at this point lay in the region 0-90 or 270-360 degrees, the plus sign was used for all spectral elements that had a phase value in the same range and the minus sign was used for all elements whose phase lay outside the region.

4. RESULTS OF I-4 DATA

The reduced data for an air mass of 1.13 is presented in Figure 47 showing some of the major atmospheric absorption bands. The spectral irradiance of the sun, assuming it to be a 6000°K blackbody, is also plotted for comparison. It can be seen that at long wavelengths the solar spectral irradiance curve falls under that of the 6000°K curve. This is of interest because in estimating the solar constant, most earlier observers had assumed the solar spectral curve in the range beyond 0.6μ to be that of a 6000°K blackbody.[1,2] It is unfortunate that data at large air masses are not available due to saturation of the instrument when operated with a lower attenuation. This problem illustrates the major drawback of Fourier spectroscopy—the results are not immediately available in time to detect and correct such difficulties. However, in the infrared region of the spectrum the transmittance of the atmospheric "windows" is nearly 100% so that an envelope of the reduced curve can be considered a zero air mass curve.

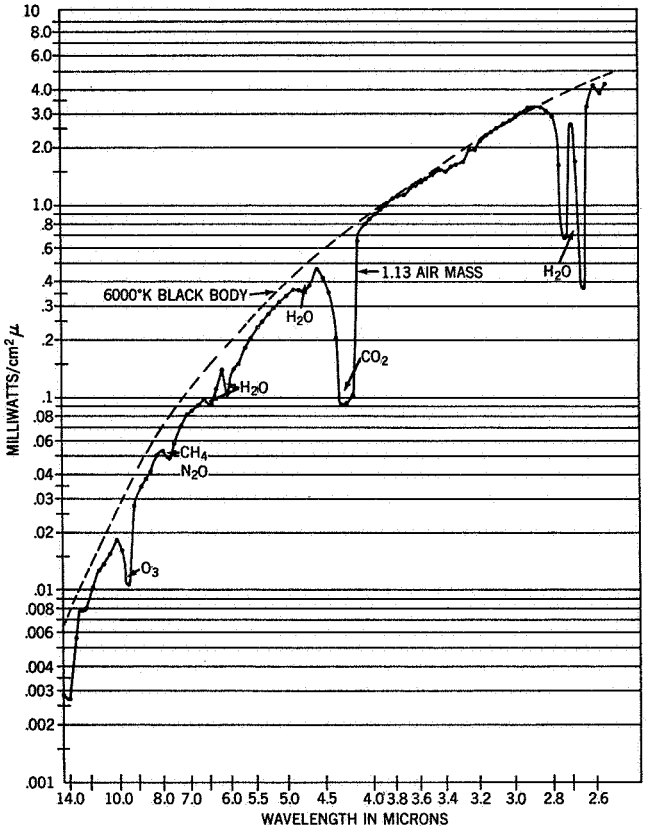

Figure 47—Solar spectrum at air mass 1.13, I-4 Interferometer

5. P-4 DATA ANALYSIS AND RESULTS

Selected portions of the P-4 interferograms have been reduced. In the photomultiplier range where the solar spectrum is several orders of magnitude stronger than that of the standard lamp, the absolute calibration of the instrument seemed to yield large uncertainties. Since this region is adequately covered by the monochromators we shall restrict ourselves here to the analysis of the data in the PbS range.

For the analysis of the data from the lead sulfide detector, 14 spectral scans of the sun and 7 spectral scans of the standard lamp were used. Each scan was the result of coadding about 40 spectra obtained by Fourier transform of a large number of interferograms. The 14 solar spectra were distributed among the following flights, 2 from August 3, 4 from August 8, 7 from August 10, and 1 from August 16. Of the calibration runs one was from interferograms made during the flight and the rest from those made later at GSFC. The air mass for the solar spectra varied from 1.13 to 5.10. The print out data of the computerized Fourier transform give for each frequency value of the spectrum a value of the spectral amplitude S, and of the logarithm to the base 10 of S. It was found that the log S values were more convenient for mathematical computations. Values of log S in the frequency range 81 to 280, λ 2.202 to .7236μ, were tabulated from each of the solar and calibration spectra and for 120 of the computer generated frequency values. The log P values outside this range were considered less reliable due to the high noise to signal ratio. The conversion of frequency to wavelength is performed by means of the equation $f\lambda = (n_e - n_o)\, k$ where f is the frequency, λ is the wavelength, n_e and n_o are the extraordinary and ordinary indices of refraction of quartz, the material of the soleil prism, and k is a constant to be determined empirically. For our instrument k had been found to be 2.2607×10^8 Å sec^{-1}. In practice for more accurate interpolation, the wavenumber was computed from a previously prepared table and the reciprocal was taken at each frequency.

The spectral irradiance P is related to the spectral amplitude S by the equation

$$\log P_S = \log P_L + \log S_S - \log S_L \qquad (15)$$

where the subscripts S and L denote the sun and the standard lamp respectively. The values are available on a relative scale only, since calibration runs were made at different distances of the lamp from the P-4, and the factors due to angular aperture, etc., could not be determined with sufficient accuracy. Comparison of log S_L values from different spectra showed that while the absolute values for any given λ varied over a wide range, (1.8 to 0 on the log scale or a factor of over 60) the differences between corresponding values of any two spectra were highly constant, independent of frequency, thus establishing the validity of Equation (15). The wavelength resolution varies from 15 A at .72μ to 170 A at 2.2μ. For each of the 120 selected wavelengths the average log S_L from the 7 calibration scans and the average log S_S from the 14 solar scans were computed. Since log S_S varies linearly with air mass the average log S_S is the value corresponding to the average air mass, namely 2.719. To determine log S_S for zero air mass the values of log S_S for each spectral scan and wavelength were plotted as a function air mass. Although the points showed a wide scatter, due partly to the process of normalization, there was a clear indication of the slope of the line of log S_S versus air mass increasing to a maximum at each of the well known H_2O absorption bands. A significant result is that even in the so-called atmospheric windows, far from the absorption bands, the slope does not become zero; there is a continuum absorption which for unit air mass at 38,000 feet is about half a percent. Figure 48 shows the results of these studies. The slope of the lines were plotted as a function of wavelength and a smooth curve was drawn through the observed points. The Y-axis was scaled to show the transmittance of the atmosphere

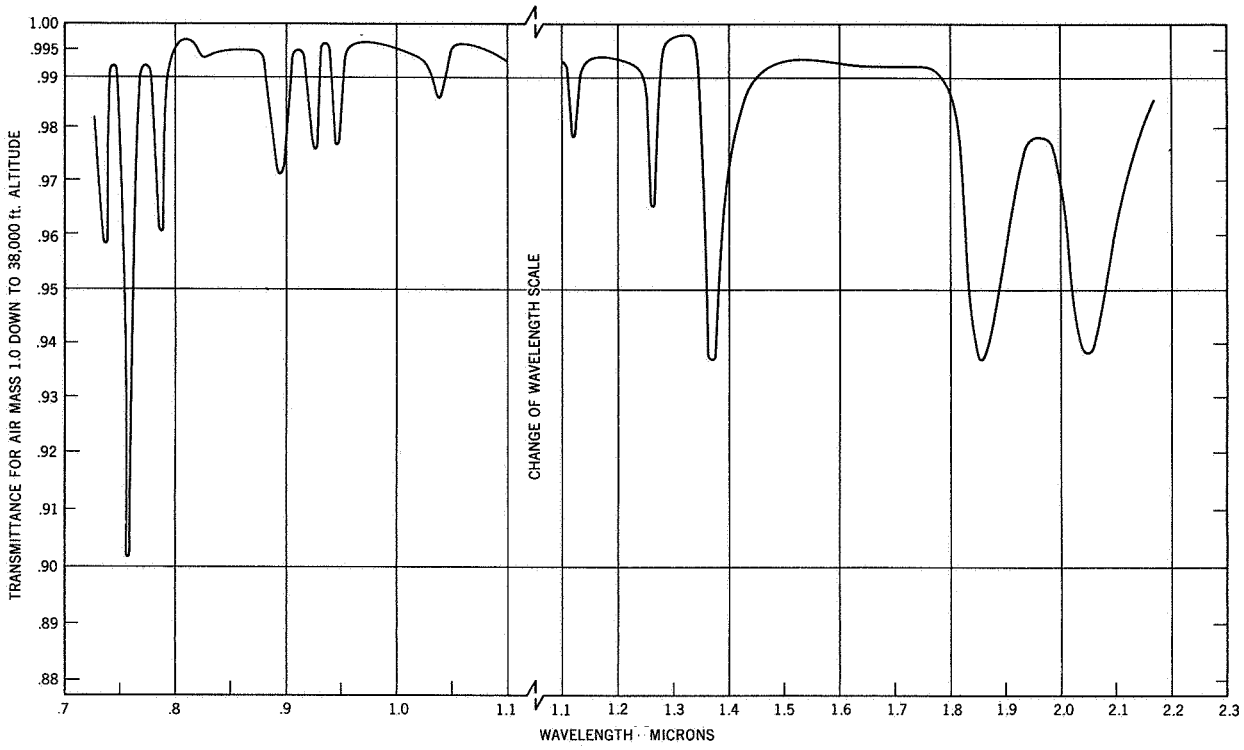

Figure 48—Transmittance of the atmosphere for Air Mass I down to 38,000 in the range 0.7 to 2.3 μ, based on P-4 data.

down to the aircraft altitude of 38,000 ft for normally incident solar radiation, that is, the ratio of solar spectral irradiance at 38,000 ft to that for zero air mass. This curve represents the average effect of the 14 P-4 interferometer scans which were analyzed.

5a. Analysis of Water Vapor Absorptance

A comparison of Figure 48 with the lowest of the four curves in Figure 8 shows many similar features. The absorption dips occur at the same wavelengths. Except for one absorption band due to O_2, the rest are due to atmospheric water vapor. The high wavelength resolution of the P-4 shows considerably more detail. At the two wavelengths near 1.4 and 1.9μ where the transmittance of the atmosphere down to ground level as shown in Figure 8 is zero, the transmittance down to the aircraft altitude is about 94%. There is also a great difference in the width and transparency of the atmospheric windows as shown in Figure 8 and 48. The absorptance of about 1/2 percent in these windows as shown in Figure 48 is due to the wings of the H_2O bands, but more significantly to the Rayleigh and aerosol scattering, as seen from a comparison of the observed values with the theoretical values of Table 3.

As stated earlier the transmittance curve of Figure 48 represents an average of several flights. Too few scans of the P-4 have been analyzed to yield a more detailed data of the variations in the H_2O content above the aircraft for different dates and locations. The Perkin-Elmer data analyzed by the computer and integrated over wide wavelength bands also failed to show the finer details of H_2O absorption. As shown in Part II, Section A, total irradiance as measured by the cone radiometer gave clear evidence of increased atmospheric absorption at certain locations. A

more careful study of the Leeds and Northrup charts of the Perkin-Elmer showed a correlation with the cone data. In order to obtain quantitative data on the amount of precipitable water vapor above the aircraft, a series of measurements were made in the laboratory to determine the absorption profiles of the water bands in the range 1.2 to 3.4 μ. The Perkin-Elmer monochromator was used with the 2 mm slit width as for the solar measurements on board NASA 711. The source was a 1000 w quartz iodine lamp. The beam was rendered parallel by a concave mirror, travelled a measured distance in clean, dust-free air of known relative humidity, and then was focussed on the entrance slit of the monochromator. Measurements were made for several pathlengths and the absorptance curves were normalized to 28 microns of precipitable water vapor (N.T.P.). The results are presented in Figure 49. The temperature and relative humidity in the laboratory were such that the amount of precipitable water vapor per meter of path length was 7 microns.

The absorption band near 1.8 μ was measured on a large number of the Leeds and Northrup charts made with the Perkin-Elmer on board NASA 711. The 2.7 μ band had been covered only on the flight of August 16. Computations based on these measurements and the laboratory data of Figure 49 showed that in general the amount of precipitable water vapor above 38,000 ft varies with latitude, not with longitude. Along the path of the transit flight of August 16, the water vapor was 28μ, while an increase from 10μ to near 28μ, was observed during the sunrise flight of August 10. On the other hand very high values of water vapor, above 40μ, were observed during the early part of the flights of August 14 and 19.

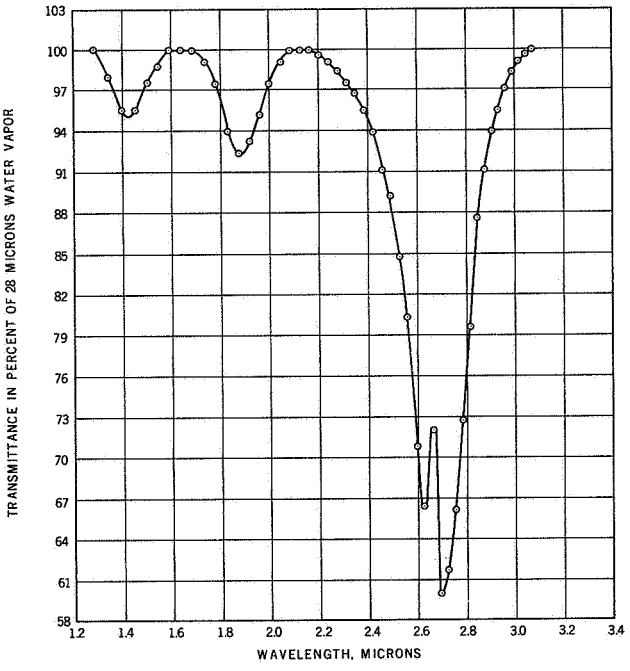

Figure 49—Transmittance of 28 microns of precipitable water vapor based on laboratory measurements with a Perkin-Elmer monochromator.

5b. Spectral Irradiance from P-4

The average value of log S_s (signal from the sun) as obtained from the P-4 was tabulated for 120 wavelengths in the spectral range .7236 to 2.202μ, it was corrected for the attenuation due to air mass 2.719, and by applying Equation (15), log P_s (solar irradiance) was computed. These values are on a relative scale since a limiting diaphragm had been mounted in front of the integrating sphere of the P-4, and that made an absolute calibration on board NASA 711 with reference to the standard lamp impossible. The diaphragm prevented the P-4 from viewing all of the standard lamp. The relative scale of the solar spectral irradiance was changed to an absolute scale by two methods. The Perkin-Elmer data in the thermocouple range were analyzed using a manual method at a large number of wavelength with due corrections for scattered light from the roof of the plane and atmospheric attenuation. The energy in the range of the P-4, PbS detector was made to agree with that given by the Perkin-Elmer. A further slight adjustment was made

when a composite curve of solar spectral irradiance based on all the spectral measurements was obtained and the area under the curve was made to agree with the weighted value of the solar constant as given by the total irradiance instruments. The normalized values of the spectral irradiances at each of the 120 selected wavelengths are indicated by the black dots in Figure 29.

CONCLUSION

M. P. Thekaekara

The following are the values of the solar constant as measured by the four total irradiance instruments on board NASA 711 Galileo at 38,000 ft in August 1967.

Cone radiometer	135.8 ± 2.4 mw cm^{-2}.
Hy-Cal pyrheliometer	135.2 ± 2.2 mw cm^{-2}.
Ångström pyrheliometer (6618)	134.3 ± 2.6 mw cm^{-2}.
Ångström pyrheliometer (7635)	134.9 ± 4.0 mw cm^{-2}.

These values are in agreement, within the range of the estimated errors of the respective instruments. An arithmetical average yields 135.05 mw cm^{-2}. A weighted average, assuming for each instrument a weight inversely proportional to the estimated error, yields 135.08 mw cm^{-2}. We accept 135.1 mw cm^{-2} as the value for the solar constant. The estimated error is ±2.8 mw cm^{-2}. Assuming for the mechanical equivalent of heat 4.186 joules/cal, the solar constant is 1.936 ± .041 calories cm^{-2} min^{-1}. This is 3.3% lower than Johnson's value, 2.00 cal cm^{-2} min^{-1}, but closer to two recently published values, 1.95 cal cm^{-2} min^{-1} given both by Stair and Ellis,[31] and by Drummond, Hickey, Scholes and Laue.[34]

We give below a table (Table 6) of values of spectral irradiance of the sun for zero air mass and for the average sun-earth distance, and a solar spectral irradiance curve (Figures 50 and 51) which displays graphically the values of Table 6. The wavelength covered by our measurements is 0.3 to 15μ, but for the sake of completeness and for obtaining an integrated value of the solar constant, the table of values has been extended to .14μ in the UV and to 20μ in the IR. For $\lambda < 0.3\mu$ an expanded scale has been used for both wavelength and irradiance, and in Figure 51 different scales are used for irradiance in three wavelength ranges. The integrated area under the curve is 135.1 mw cm^{-2}, the value obtained from the total irradiance instruments.

In the wavelength range 0.3 to 2.2μ which accounts for all but 6.4 percent of the energy of the sun, our values are based on four instruments, the two monochromators, Perkin-Elmer and Leiss, the filter radiometer and the P-4 interferometer though not all of them cover the whole range. The agreement between the instruments is within the estimated errors of each. The differences are small except in the range 0.4 to 0.7μ where the ratio of the spectral irradiance of the sun to that of the standard lamp is very high. In this range the Perkin-Elmer values are higher than those of

Table 6

Solar Spectral Irradiance (Based on Measurements on Board NASA-711 "Galileo" at 38,000 feet) λ—wavelength in microns; P_λ—Solar Spectral Irradiance averaged over small bandwidth centered at λ, in watts $cm^{-2}micron^{-1}$; D_λ—percentage of the Solar Constant associated with wavelengths shorter than wavelength λ. Solar Constant 0.13510 watt cm^{-2}.

λ	P_λ	D_λ	λ	P_λ	D_λ	λ	P_λ	D_λ	λ	P_λ	D_λ
0.140	0.0000048	0.00050	0.395	0.1191	8.189	0.630	0.1542	39.26	3.8	0.00111	98.902
0.150	0.0000176	0.00059	0.400	0.1433	8.675	0.640	0.1517	40.39	3.9	0.00103	98.982
0.160	0.000059	0.00087	0.405	0.1651	9.245	0.650	0.1487	41.50	4.0	0.00095	99.055
0.170	0.00015	0.00164	0.410	0.1759	9.876	0.660	0.1468	42.00	4.1	0.00087	99.122
0.180	0.00035	0.00349	0.415	0.1783	10.53	0.670	0.1443	43.67	4.2	0.00078	99.182
0.190	0.00076	0.00760	0.420	0.1758	11.19	0.680	0.1418	44.73	4.3	0.00071	99.238
0.200	0.00130	0.0152	0.425	0.1705	11.83	0.690	0.1398	45.78	4.4	0.00065	99.289
0.205	0.00167	0.0207	0.430	0.1651	12.45	0.700	0.1369	46.80	4.5	0.00059	99.335
0.210	0.00269	0.0288	0.435	0.1675	13.06	0.710	0.1344	47.80	4.6	0.00053	99.376
0.215	0.00445	0.0420	0.440	0.1823	13.71	0.720	0.1314	48.79	4.7	0.00048	99.414
0.220	0.00575	0.0609	0.445	0.1936	14.41	0.730	0.1290	49.75	4.8	0.00045	99.448
0.225	0.00649	0.0835	0.450	0.2020	15.14	0.740	0.1260	50.69	4.9	0.00041	99.480
0.230	0.00667	0.1079	0.455	0.2070	15.90	0.750	0.1235	51.62	5.0	0.000383	99.509
0.235	0.00593	0.1312	0.460	0.2080	16.66	0.800	0.1107	55.95	6.0	0.000175	99.716
0.240	0.00630	0.1534	0.465	0.2060	17.43	0.850	0.0988	59.83	7.0	0.000099	99.817
0.245	0.00723	0.1788	0.470	0.2045	18.19	0.900	0.0889	63.30	8.0	0.000060	99.876
0.250	0.00704	0.2053	0.475	0.2055	18.95	0.950	0.0835	66.49	9.0	0.000038	99.912
0.255	0.0104	0.2375	0.480	0.2085	19.72	1.000	0.0746	69.42	10.0	0.000025	99.935
0.260	0.0130	0.2808	0.485	0.1986	20.47	1.1	0.0592	74.37	11.0	0.0000170	99.951
0.265	0.0185	0.3391	0.490	0.1959	21.20	1.2	0.0484	78.35	12.0	0.0000120	99.962
0.270	0.0232	0.4163	0.495	0.1966	21.92	1.3	0.0396	81.61	13.0	0.0000087	99.969
0.275	0.0204	0.4960	0.500	0.1946	22.65	1.4	0.0336	84.32	14.0	0.0000055	99.975
0.280	0.0222	0.5758	0.505	0.1922	23.36	1.5	0.0287	86.62	15.0	0.0000049	99.9785
0.285	0.0315	0.6752	0.510	0.1882	24.07	1.6	0.0244	88.59	16.0	0.0000038	99.9817
0.290	0.0482	0.8225	0.515	0.1833	24.76	1.7	0.0202	90.24	17.0	0.0000031	99.9843
0.295	0.0584	1.020	0.520	0.1833	25.43	1.8	0.0159	91.58	18.0	0.0000024	99.9863
0.300	0.0514	1.223	0.525	0.1852	26.12	1.9	0.0126	92.63	19.0	0.0000020	99.9879
0.305	0.0602	1.430	0.530	0.1842	26.80	2.0	0.0103	93.48	20.0	0.0000016	99.9893
0.310	0.0686	1.668	0.535	0.1818	27.48	2.1	0.0090	94.19	λ_∞		100.0
0.315	0.0757	1.935	0.540	0.1783	28.14	2.2	0.0079	94.82			
0.320	0.0819	2.227	0.545	0.1754	28.80	2.3	0.0068	95.36			
0.325	0.0958	2.555	0.550	0.1725	29.44	2.4	0.0064	95.85			
0.330	0.1037	2.925	0.555	0.1720	30.08	2.5	0.0054	96.287			
0.335	0.1057	3.312	0.560	0.1695	30.71	2.6	0.0048	96.664			
0.340	0.1050	3.702	0.565	0.1700	31.34	2.7	0.0043	97.001			
0.345	0.1047	4.090	0.570	0.1705	31.97	2.8	0.0039	97.305			
0.350	0.1074	4.483	0.575	0.1710	32.60	2.9	0.0035	97.579			
0.355	0.1067	4.879	0.580	0.1705	33.23	3.0	0.0031	97.823			
0.360	0.1055	5.271	0.585	0.1700	33.86	3.1	0.0026	98.034			
0.365	0.1122	5.674	0.590	0.1685	34.49	3.2	0.00226	98.214			
0.370	0.1173	6.099	0.595	0.1665	35.11	3.3	0.00192	98.368			
0.375	0.1152	6.529	0.600	0.1646	35.72	3.4	0.00166	98.501			
0.380	0.1117	6.949	0.605	0.1626	36.33	3.5	0.00146	98.616			
0.385	0.1097	7.359	0.610	0.1611	36.93	3.6	0.00135	98.720			
0.390	0.1099	7.765	0.620	0.1576	38.11	3.7	0.00123	98.816			

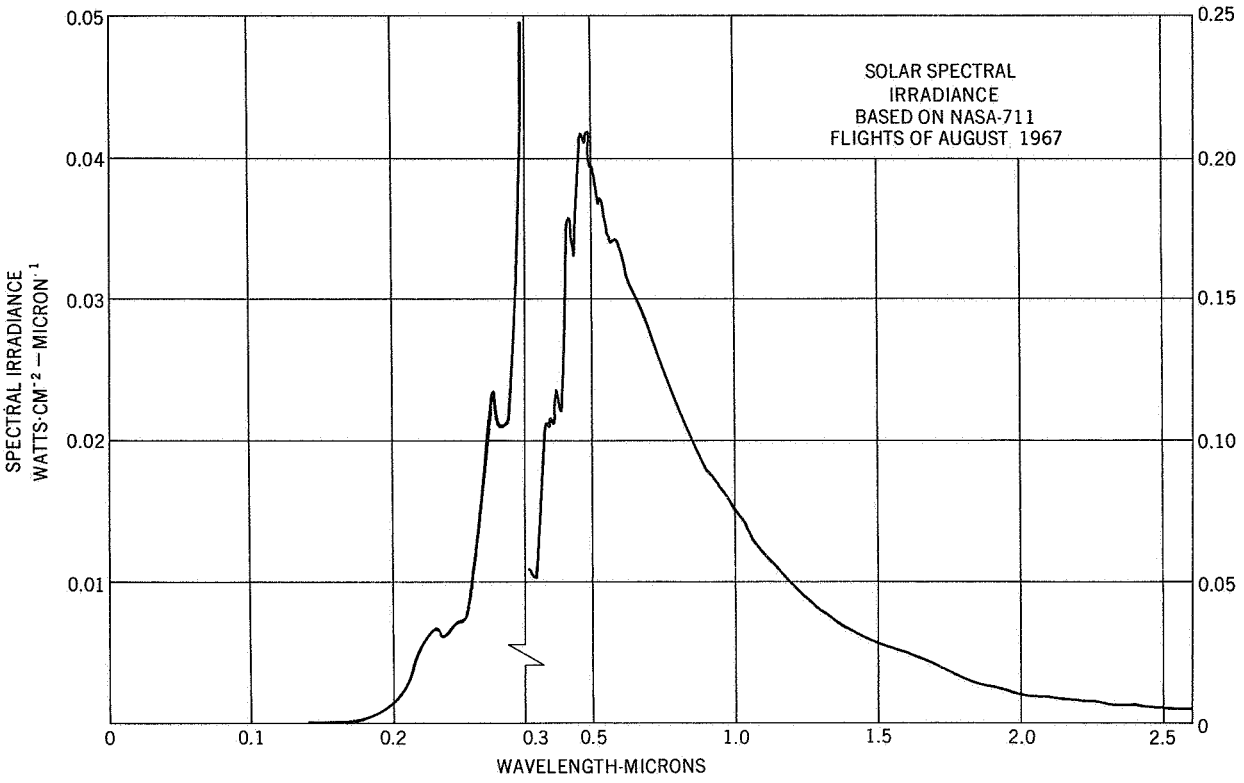

Figure 50—Solar spectral irradiance 0.14-2.5μ (based on NASA 711 flights of August 1967).

the filter radiometer. The normalized values of the Leiss are close to the latter, but the unnormalized values are close to the former. In the range 0.3 to 0.75μ the value given for each wavelength is the average irradiance for a 100 A bandwidth centered at that wavelength. This gives a solar irradiance independent of the detailed Fraunhofer structure which each instrument displays in a different way according to its wavelength resolution. In the range beyond 0.7μ where the Fraunhofer structure is small and our wavelength resolution becomes less, wider bandwidths are used for the averaging. In the range 1.0 to 5.0μ each irradiance value is the average over 1000 A. The wavelength range 2.2 to 15μ is covered by the Perkin-Elmer up to 4μ and by the I-4 from 2.6 to 15μ.

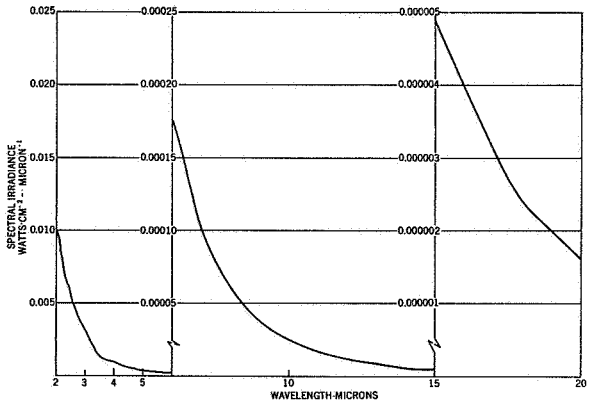

Figure 51—Solar spectral irradiance 2.5 to 20μ (based on NASA 711 flights of August 1967).

It would seem that Table 6 and Figures 50 and 51 present the first direct and detailed measurements of solar irradiance in the wavelength range longer than 0.7μ. In this range the widely accepted Johnson curve, following that of P. Moon, is as stated earlier that of a 6000°K blackbody. Our data indicate an effective blackbody temperature which decreases as the wavelength increases. This is in agreement with

measurements made at three wavelengths between 1.0 to 2.5μ by Peyturaux,[13] at 11μ by Saiedy and Goody[35] and at 6 mm by Whitehurst *et al.*[36] Our extrapolation of the curve in the range 15 to 20μ is based on this decrease of effective blackbody temperature. In preparing the final table the spectral irradiance values obtained by taking a weighted average of the data of the different instruments were scaled down by about 0.1 percent in order to obtain a solar constant in agreement with the total irradiance instruments. In the wavelength range below 0.3 where the ozone above the aircraft is an almost complete absorber we have used the rocket data of the Naval Research Laboratory as given by Detwiler, Garrett, Purcell and Tousey[37] for the range 0.14 to 0.26μ and by Johnson[1] for the range 0.26 to 0.30μ. Since our observed values in the range 0.3 to 0.4μ are 0.927 times those of Johnson, and Detwiler *et al* had adjusted their irradiance values for wavelength less 0.26μ to Johnson's scale, we have scaled the NRL values down by 7.3%.

In column 3 of Table 6 we have given D_λ, the percentage of the total solar energy associated with wavelengths from 0 to λ. The value for the first entry 0.140μ is based on Detwiler *et al.* who give the irradiance down to 0.085μ.

Our final table is based on a detailed analysis of many sets of data from a variety of instruments. Instrumental errors arise from different sources for each instrument and intercomparison of data permits to a great extent the minimizing of their effects on the final weighted average. Hence we estimate that our spectral irradiance values have an accuracy of ±5 percent.

A point by point comparison of our spectral irradiance values with those of Johnson shows that our values are lower almost everywhere, especially in the UV and visible. In two short wavelength ranges in the IR 0.9 to 1.05μ and 1.35μ to 1.9μ our values are higher, and this has partially been confirmed by the data from the Cary 14 monochromator flown by the Ames group (private communication from J. C. Arveson). The disagreement between our curve and that of Johnson is most pronounced in the range 0.52 to 0.70μ, ours being lower by as much as 12% at 0.55μ.

REFERENCES

1. F. S. Johnson, J. Meteor, *11* , 431 (1954).

2. P. Moon, J. Franklin Institute, *230*, 583 (1940).

3. L. B. Aldrich and G. C. Abbot, Smithsonian Institute, Misc. Coll., 110, No. 5 (1948).

4. W. Schuepp, (Dissertation, Basel), 1949.

5. C. W. Allen, Observatory, *70*, 154 (1950).

6. L. B. Aldrich and W. H. Hoover, Science, *116*, 3 (1952).

7. C. W. Allen, *Astrophysical Quantities*, University of London, London, England (1955).

8. R. Stair and R. G. Johnston, J. Research National Bureau Standards, *57*, 205 (1956).

9. C. W. Allen, Quarterly J. Roy. Meteor. Soc. *84*, 362, 307-318 (1958).

10. D. Deirmedjian and Z. Sekera, J. Opt. Soc. Am. *46*, 565 (1956).

11. F. S. Johnson, J. D. Purcell, R. Tousey, and N. Wilson, Rocket Exploration of the Upper Atmosphere, Ed. Boyd and Seaton (Pergamon Press, London, 1954), p. 279.

12. E. Makarova, Astron. Zhurnal., *34*, 539 (1957).

13. R. Peyturaux, Ann. d'Astrophys., *15*, 302 (1952).

14. D. Labs., Z. Astrophys. *44*, 37 (1957).

15. P. R. Gast, in *Handbook of Geophysics*, C. F. Campen, Jr., *et alii*, ed., Pp. 16-14 to 16-30, (McMillan Co., New York, 1960).

16. L. Dunkelman and R. Scolnik, J. Opt. Soc. Am., *49*, 356 (1959).

17. M. P. Thekaekara, "Survey of the Literature on the Solar Constant and the Spectral Distribution of Solar Radiant Flux," NASA, Washington, D. C., 1965, SP-74. M. P. Thekaekara, Solar Energy, *9*, 7-20 (1965).

18. R. B. Toolin, "Atmospheric Optics" in *Handbook of Geophysics and Space Environments*, S. L. Valley, Ed., McGraw Hill Book Co., New York (1965) pp 7-12 to 7-35.

19. "Solar Instrumentation Installation in Convair 990A Aircraft" Report. NASA Goddard Contract NAS-5-3744, Fairchild-Hiller Corp., Germantown, Md., (1967).

20. M. Gutnik, "Atmospheric Water Vapor," in *Handbook of Geophysics and Space Environments*, S. L. Valley, Ed., McGraw Hill Book Co., N.Y., (1965) pp. 3-37.

21. U. S. Nautical Almanac Office, *The American Ephemeris and Nautical Almanac for the Year 1967*, U. S. Gov't. Printing Office, Washington, D. C. (1965) *passim*.

22. A Bemporad, Meteorologische Zeitschrift, *24*, 306 (1907).

23. F. Kasten, "A New Table and Approximation Formula for the Relative Optical Air Mass," Tech. Report 136, Cold Regions Research and Engineering Laboratory, Hanover, N. H., (1964) (AD610554).

24. A. Gouffé, Rev. Opt. *24*, Nos 1-3 (1945).

25. P. Campanaro and T. Ricolfi, J. Opt. Soc. Am. *57*, 1 (1967).

26. A. Ångström, Tellus 3 (1961)—Reprint Series No. F6, Eppley Foundation for Research, Newport, R. I.

27. R. Stair et alii, NASA CR-201, NASA, Washington, D. C., 1965, p. 44.

28. T. S. Moss, *Optical Properties of Semiconductors,* (Butterworth's Scientific Publications, London, England, 1959), p. 7.

29. M. Minnaert, G. F. W. Mulders, and J. Houtgast, *Photometric Atlas of the Solar Spectrum,* D. Schnabel, Amsterdam, 1940.

30. R. Stair, W. E. Schneider and J. K. Jackson, Appl. Optics *2*, 1151 (1963).

31. R. Stair and H. T. Ellis, "The Solar Constant Based on New Spectral Irradiance Data from 3100 to 5300 Ångströms" J. of Appl. Meteorology, Aug (1968).

32. R. Stair, "Preliminary Report on the Measurement of Spectral Solar Radiation with a Photoelectric Filter Radiometer on Six CV-990 Flights During August 1967," NASA, Goddard Contract NAS 5-9488.

33. J. Webb, "An Electronic Scanning Spectrometer for UV Measurements," GSFC, X-713-67-108, 1967 p. 6.

34. A. J. Drummond, J. R. Hickey, W. J. Scholes and E. G. Laue, J. of Spacecraft and Rockets, *4*, 1200 (1967).

35. F. Saiedy and R. M. Goody, Monthly Not. Roy. Astron. Soc. *119* No. 3, 17 (1959).

36. R. N. Whitehurst, J. Copland and F. H. Mitchell, J. App. Phys. *28*, 295 (1957).

37. C. R. Detwiler, D. L. Garrett, J. D. Purcell and R. Tousey, Ann. Geophys. *17*, 9 (1961).